Geochemistry Geophysics Geosystems G3

Article
Volume 15, Number 1
23 January 2014
doi: 10.1002/2013GC004861
ISSN: 1525-2027

Published by AGU and the Geochemical Society

Finite-frequency Rayleigh wave tomography of the western Mediterranean: Mapping its lithospheric structure

I. Palomeras, S. Thurner, A. Levander, and K. Liu
Department of Earth of Earth Science (MS126), Rice University, 6100 Main St., Houston, Texas 77005, USA (imma.palomeras@gmail.com)

A. Villasenor and R. Carbonell
Department of Earth's Structure and Dynamics, Institute of Earth Sciences "Jaume Almera," Barcelona, Spain

M. Harnafi
Department of Earth Sciences, Université Mohammed V, Rabat, Morocco

[1] We present a 3-D shear wave velocity model for the crust and upper mantle of the western Mediterranean from Rayleigh wave tomography. We analyzed the fundamental mode in the 20–167 s period band (6.0–50.0 mHz) from earthquakes recorded by a number of temporary and permanent seismograph arrays. Using the two-plane wave method, we obtained phase velocity dispersion curves that were inverted for an isotropic Vs model that extends from the southern Iberian Massif, across the Gibraltar Arc and the Atlas mountains to the Saharan Craton. The area of the western Mediterranean that we have studied has been the site of complex subduction, slab rollback, and simultaneous compression and extension during African-European convergence since the Oligocene. The shear velocity model shows high velocities beneath the Rif from 65 km depth and beneath the Granada Basin from ~70 km depth that extend beneath the Alboran Domain to more than 250 km depth, which we interpret as a near-vertical slab dangling from beneath the western Alboran Sea. The slab appears to be attached to the crust beneath the Rif and possibly beneath the Granada Basin and Sierra Nevada where low shear velocities (3.8 km/s) are mapped to >55 km depth. The attached slab is pulling down the Gibraltar Arc crust, thickening it, and removing the continental margin lithospheric mantle beneath both Iberia and Morocco as it descends into the deeper mantle. Thin lithosphere is indicated by very low upper mantle velocities beneath the Alboran Sea, above and east of the dangling slab and beneath the Cenozoic volcanics.

Components: 11,497 words, 13 figures.

Keywords: western Mediterranean; Rayleigh wave tomography; subduction.

Index Terms: 7218 Lithosphere: Seismology; 7240 Subduction zones: Seismology; 7255 Surface waves and free oscillations: Seismology; 7270 Tomography: Seismology; 1207 Transient deformation: Geodesy and Gravity; 1219 Gravity anomalies and Earth structure: Geodesy and Gravity; 1236 Rheology of the lithosphere and mantle: Geodesy and Gravity; 1240 Satellite geodesy: results: Geodesy and Gravity; 6982 Tomography and imaging: Radio Science; 8180 Tomography: Tectonophysics.

Received 28 May 2013; **Revised** 9 December 2013; **Accepted** 12 December 2013; **Published** 23 January 2014.

Palomeras, I., S. Thurner, A. Levander, K. Liu, A. Villasenor, R. Carbonell, and M. Harnafi (2014), Finite-frequency Rayleigh wave tomography of the western Mediterranean: Mapping its lithospheric structure, *Geochem. Geophys. Geosyst.*, *15*, 140–160, doi:10.1002/2013GC004861.

1. Introduction

[2] The Mediterranean has been affected by slow oblique compression due to African-European convergence since the Cretaceous, with the Tethyan oceanic lithosphere being recycled into the mantle beneath Europe [e.g., *Royden*, 1993]. The western Mediterranean now comprises a convergent diffuse plate boundary between the African and the Eurasian plates with deformation extending from the Betic Mountains in southern Spain, to as far south as the High Atlas in Morocco (Figure 1a). Although the region is a convergent margin, parts of it have experienced extension since Oligocene times when the convergence speed between Africa and Eurasia decreased and widespread slab rollback started throughout the Mediterranean [*Malinverno and Ryan*, 1986; *Royden*, 1993; *Wortel and Spakman*, 2000; *Faccenna et al.*, 2004]. Slab retreat formed the modern Mediterranean basins including the Aegean, Tyrrhenian, Ligurian, and Alboran Sea as well as the Valencia Trough [e.g., *Durand et al.*, 1999]. Current African movement with respect to Eurasia is to the northwest at 3–4 mm/yr in North Africa, rotating to a more westerly direction in the Gibraltar Strait [*Koulali et al.*, 2011].

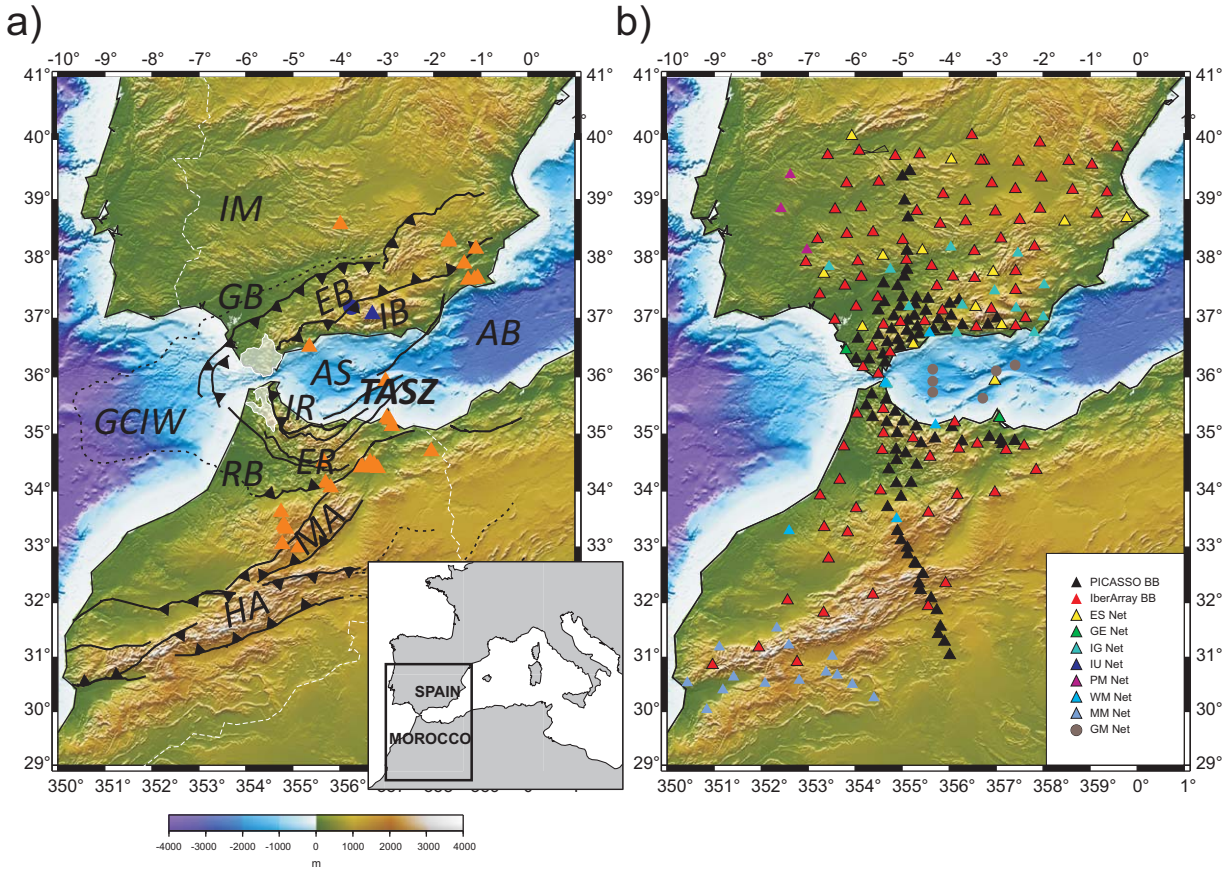

Figure 1. (a) Elevation map of the western Mediterranean with the principal tectonic units and (b) the stations used in this study. (Figure 1a) The main tectonic unit of the Iberian Peninsula is the Iberian Massif (IM) in the north and west of the study area. In the southwest of Spain are the Betic Mountains, composed of the Internal Betics (IB) and External Betics (EB). The Guadalquivir Basin (GB) is the Betic foreland basin. The equivalent to the Betics in Morocco are the Rif Mountains consisting of the Internal Rif (IR) and the External Rif (ER). The associated foreland basin is the Rharb Basin (RB). The Internal Betics (IB), Internal Rif (IR), and Alboran Sea (AS) constitute the Alboran Domain, while the Betics and Rif combined form the Gibraltar Arc. The white shadow area represents the Flysch Domain. West of the Gibraltar Strait is the Gulf of Cadiz Imbricate Wedge (GCIW). In the south of the study area are the Middle Atlas (MA) and High Atlas (HA) Mountains. Blue triangle and circle indicate the position of Sierra Nevada and the Granada Basin, respectively. The Cenozoic volcanic fields are represented by orange triangles. (Figure 1b) The broadband stations and the different networks used for this study.

[3] Different, but not exclusive models have been proposed to explain the geology of the Alboran Sea and Gibraltar Arc regions and reconstruct their tectonic evolution. The models can be grouped in two major themes: slab rollback scenarios and mantle lithosphere instabilities with or without continental lithosphere delamination. A large number of contributions describe variations on these two main themes, based on geologic, geodynamic, seismologic, and other evidence [e.g., *Platt and Vissers*, 1989; *Royden*, 1993; *Calvert et al*., 2000; *Gutscher et al*., 2002, 2012, and references therein].

[4] The Atlas Mountains are an intercontinental belt in northwest Africa. This range reaches elevations higher than 2000 m with relatively minor shortening [*Beauchamp et al*., 1999; *Teixell et al*., 2003; *Arboleya et al*., 2004]. The cause of the high elevations and the relation of the uplift of this mountain belt to contemporaneous subduction and slab retreat in the Mediterranean are unclear.

[5] A variety of seismic images made largely with permanent seismic stations in Spain and Morocco and small deployments of portable instruments have displayed different aspects of the upper mantle structure in the western Mediterranean. These images, of varying quality, have been made with ray and finite-frequency teleseismic *P* wave travel time tomography [*Blanco and Spakman*, 1993; *Calvert et al*., 2000; *Wortel and Spakman*, 2000; *Piromallo and Morelli*, 2003; *Spakman and Wortel*, 2004], surface wave tomography [*Peter et al*., 2008; *Schivardi and Morelli*, 2009], and adjoint tomography [*Zhu et al*., 2012]. To better resolve the complex structures in this region, several loosely affiliated projects were started between 2007 and 2009, including the Spanish IberArray and SIBERIA broadband seismic arrays [*Díaz et al*., 2009], and the PICASSO (Program to Investigate Convective Alboran Sea System Overturn) project, which includes researchers from a variety of institutions in the U.S., Ireland, Spain, and Morocco. Subsequently, groups from German and English institutions have deployed broadband seismographs in the area, expanding the seismic footprint. The PICASSO seismology program includes an 85 element broadband seismic array deployed in a roughly north-south line from the Iberian Massif in central Spain, across the Betics, the Gibraltar Strait, the Rif Mountains, the Middle Atlas, and the High Atlas and ending on the Sahara Platform (Figure 1). Part of the PICASSO stations were also deployed in aerial arrays around the Alboran Sea in the Betic and Rif Mountains to increase the density of the more regionally distributed IberArray and SIBERIA arrays. The IberArray and SIBERIA are dense areal traveling seismic networks (interstation spacing < 60 km), which will gradually cover Spain and northern Morocco, respectively (http://iberarray.ictja.csic.es/). PICASSO, the Spanish arrays, and the existing permanent network total almost 240 broadband seismographs in our study area (Figure 1b).

[6] In this paper, we describe the analysis and interpretation of fundamental mode Rayleigh waves across the western Mediterranean. We have developed a 3-D shear velocity model from the central Iberian Peninsula in the north, to the Saharan Platform in the south. The 3-D shear velocity model integrated with other geological and geophysical data provides constraints on the different tectonic scenarios of the region. In particular, our results show evidence of an attached slab beneath the Rif and the Gibraltar Strait extending into the asthenosphere beneath the Alboran Domain. The surface wave image complements the slab imaged in the upper mantle extending into the transition zone in recent body wave tomography results [*Bezada et al*., 2013]. Lithospheric mantle is thin or absent beneath regions of Cenozoic volcanism, and beneath the eastern High and the Middle Atlas Mountains, supporting the models developed for this region [*Teixell et al*., 2005; *Zeyen et al*., 2005].

2. Geological and Geophysical Setting

[7] The northern part of the study area belongs to the stable Iberian Massif (Figure 1a). It is the southernmost exposed element of the European Variscan Belt, a Late Paleozoic orogen resulting from the collision between Gondwana and Laurasia that formed the Pangaean supercontinent [*Matte*, 1986, 2001]. The Moho depth, well constrained by active seismic profiles, is almost constant at 30–32 km depth [*Surinach and Vegas*, 1988; *Simancas et al*., 2003; *Palomeras et al*., 2009; *Martínez Poyatos et al*., 2012]. Models derived from geopotential fields provide an estimate of the lithosphere-asthenosphere boundary at ~100 km depth in western Iberia [*Fernàndez et al*., 2004; *Fullea et al*., 2010; *Palomeras et al*., 2011] deepening to ~120 km toward the Gulf of Cadiz.

[8] The central part of the sampled area comprises the westernmost segment of the Alpine-Mediterranean belt represented by the Betics in

southern and southeastern Iberia and the Rif Mountains in northern Morocco (Figure 1a). The Betics and Rif Mountains together comprise the Gibraltar Arc, an arcuate belt that partially encircles the Alboran Sea. The Guadalquivir and Rharb basins are the associated foreland basins in Spain and Morocco, respectively. Three different geologic domains can be distinguished in the Betic and Rif Mountains (Figure 1a): the Flysch Domain, the Internal Zone, and the External Zone. Active source seismic studies in the Betic Mountains [*Carbonell et al*., 1998] show a Moho depth of ~30 km, shallowing beneath the coast to 23–25 km depth. A deeper Moho, ~38 km depth, is observed beneath the Sierra Nevada mountains, where the highest peak, the Mulhacen, reaches 3479 m [*Díaz and Gallart*, 2009, and references therein]. A recent refraction/reflection experiment in the Rif Mountains [*Gallart et al*., 2012] reveals a thick crust (Moho at ~55 km depth) beneath the western Rif and thinning eastward to 25 km depth. The same results are observed by a receiver functions study that suggests a ~55 km depth Moho beneath the Gibraltar Arc [*Thurner et al*., in press].

[9] The Internal Zones, jointly with the Alboran Sea crust, are termed the Alboran Domain, an allochthonous unit that separated from the eastern Iberian margin and drifted to its current position during Cenozoic subduction rollback [e.g., *Rosenbaum et al*., 2002]. The Alboran Sea is underlain by extended continental crust, with a thickness ranging from 15 to 20 km [*Díaz and Gallart*, 2009].

[10] Moderate, shallow to intermediate (0–150 km) depth seismicity is observed in and around the Gibraltar Arc [*Grimison and Chen*, 1986; *Buforn et al*., 1991]. There is a gap with no seismicity at depths between ~150 and 600 km, with some events at depths greater than 600 km (620–660 km) almost directly beneath Granada, Spain [*Buforn et al*., 1991]. Seismic tomography images [*Gutscher et al*., 2002; *Spakman and Wortel*, 2004; *Bezada et al*., 2013] show a high velocity anomaly descending from W to E, nearly vertically beneath the Alboran Sea and reaching the mantle transition zone beneath southernmost Spain. The images also show a low velocity anomaly beneath the western Alboran Sea between 50 and 100 km [*Seber et al*., 1996a; *Morales et al*., 1999] suggesting that this high velocity anomaly is not connected to the surface. The origin of this high-velocity body has been differently interpreted as east dipping subduction [*Lonergan and White*, 1997; *Gutscher et al*., 2002; *Spakman and Wortel*, 2004], lithospheric delamination [*Seber et al*., 1996a; *Calvert et al*., 2000], and convective removal of thickened lithosphere [*Platt and Vissers*, 1989]. Several studies have been done to test these hypotheses, such as SKS splitting analysis along the Gibraltar Arc [*Buontempo et al*., 2008; *Díaz et al*., 2010] and body wave dispersion analysis under Gibraltar [*Bokelmann et al*., 2011]. The rotation along the arc of the fast polarization direction and the observed dispersion of the arrivals coming from the east in the Gibraltar area suggest that fast slab rollback is the best model to explain the geodynamics of the Alboran region, ruling out any mantle lithosphere instability model.

[11] South of the Rif Mountains there are the Middle and the High Atlas belts (Figure 1a) which are the highest mountains in Morocco. This belt, formed on a Mesozoic rift that closed during the Cenozoic Alpine orogeny [*Jacobshagen et al*., 1988; *Laville et al*., 2004], has a mean altitude of 2000 m, reaches elevations higher than 4000 m, but has experienced relatively little (<25%) shortening [*Beauchamp et al*., 1999; *Teixell et al*., 2003; *Arboleya et al*., 2004]. The average crustal thickness is 35 km on the Western High Atlas [*Timoulali and Meghraoui*, 2011]. Same thickness is observed on the High and the Middle Atlas with no significant crustal root beneath the High Atlas [*Ayarza et al*., n.d.; *Schwarz and Wigger*, 1988; *Wigger et al*., 1992]. The minor tectonic thickening observed in this mountain belt cannot explain the observed elevation, indicating that this belt is isostatically uncompensated by crustal thickness. Modeling studies using Bouguer gravity, geoid elevation, surface heat flow, and topography suggest a lithosphere thinned to <70 km depth beneath the High Atlas in order to support the observed elevation [*Teixell et al*., 2005; *Zeyen et al*., 2005; *Missenard et al*., 2006; *Fullea et al*., 2010; *Jiménez-Munt et al*., 2011].

[12] Volcanic activity has been widespread in the Atlas. The oldest extrusives, found in the High Atlas, are basalts associated with Mesozoic rifting. Paleogene to Quaternary alkaline basalts erupted in the Middle Atlas and along the southern border of the Western High Atlas. Middle and Late Miocene, Pliocene, and Quaternary volcanic units are also found in the Alboran basin, Southern Iberia, and North Africa. The composition of these units changes in time and space from calc-alkaline in southern Spain and the Alboran Sea during the Miocene, to alkali basalts in North Africa during the Pliocene and Quaternary [*Duggen et al*., 2004]. In the Iberian Massif of central Spain, Late

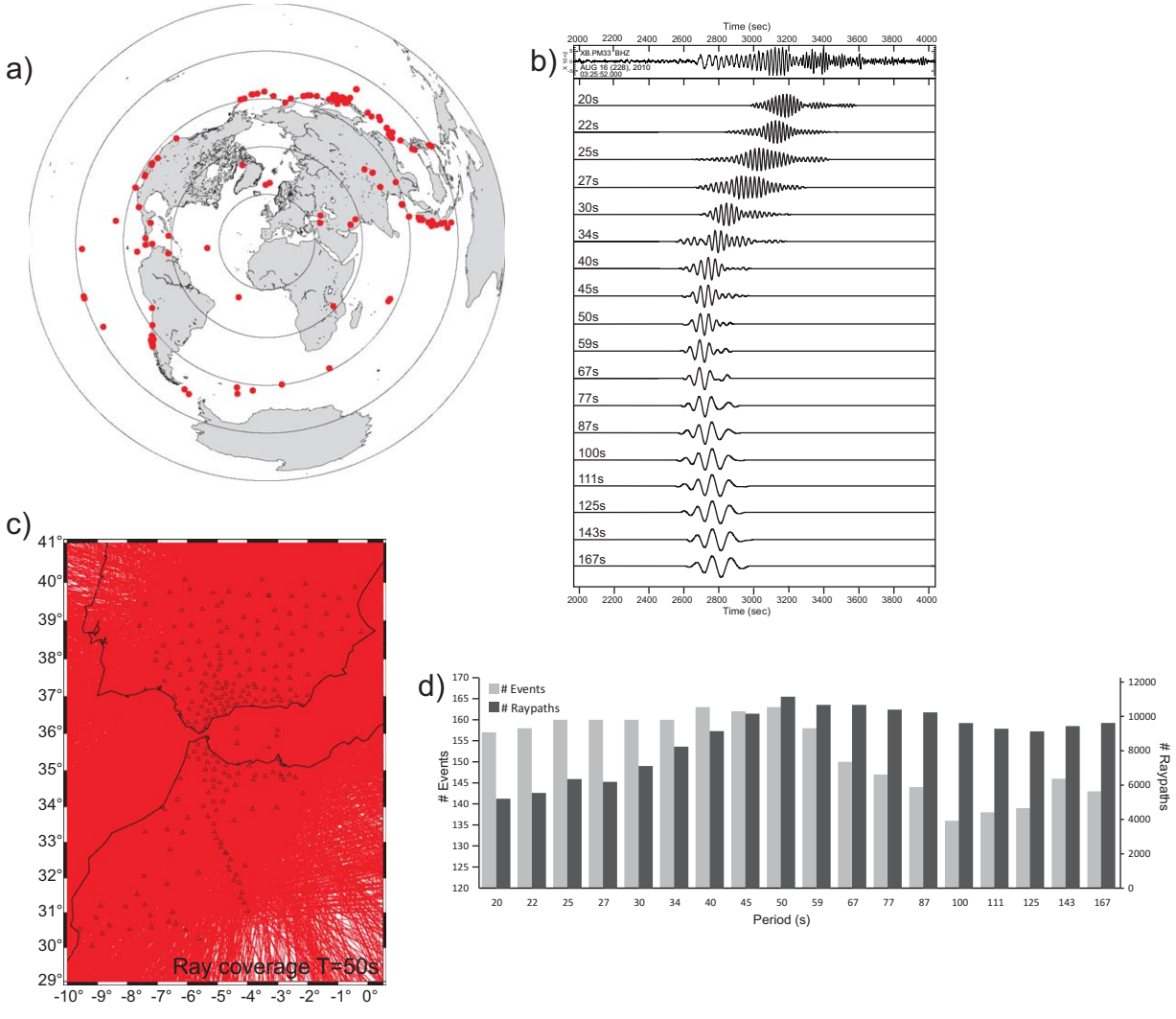

Figure 2. (a) Azimuthal distribution of earthquakes (red dots) used in this study. The concentric circles are in 30° increments centered on the study area. (b) Example of fundamental model Rayleigh waveform. (top) Vertical component of the raw data of an earthquake on 16 August 2010 (magnitude 6.3; depth 9.8 km) recorded at station XB.PM33 (epicentral distance: 82.95°). Beneath it there are the 18 different filtered frequency bands. (c) Ray coverage (red lines) in the study area for 50 s period. Open triangles are the stations used in this study. (d) Number of events and raypath used per period.

Miocene-Quaternary volcanics created the Calatrava Volcanic Province (Ciudad Real), intracontinental volcanism that has been related to extensional tectonics [*López-Ruiz et al.*, 1993].

3. Data and Methodology

[13] The data used in this paper was recorded by 228 stations belonging to different projects and institutions, including the US PICASSO project and the Spanish TopoIberia project (http://iberarray.ictja.csic.es/) (Figure 1b). We have analyzed 168 teleseismic events with magnitude greater than 6.0 and epicentral distances from the study area between 30° and 120°, recorded between April 2009 and 2011. The good azimuthal distribution of events and the number and distribution of stations provide a dense ray coverage (Figure 2a) allowing for good resolution of lateral fluctuations in phase velocity measurements. We processed the vertical component of these seismograms to isolate the Rayleigh wave signal. First, the seismograms were corrected for instrument response and filtered with Butterworth band-pass filters with 10 mHz bandwidth at 18 center periods (frequencies) from 20 to 167 s (6.0–50.0 mHz). After rejecting traces with a low signal-to-noise ratio, the surface waves

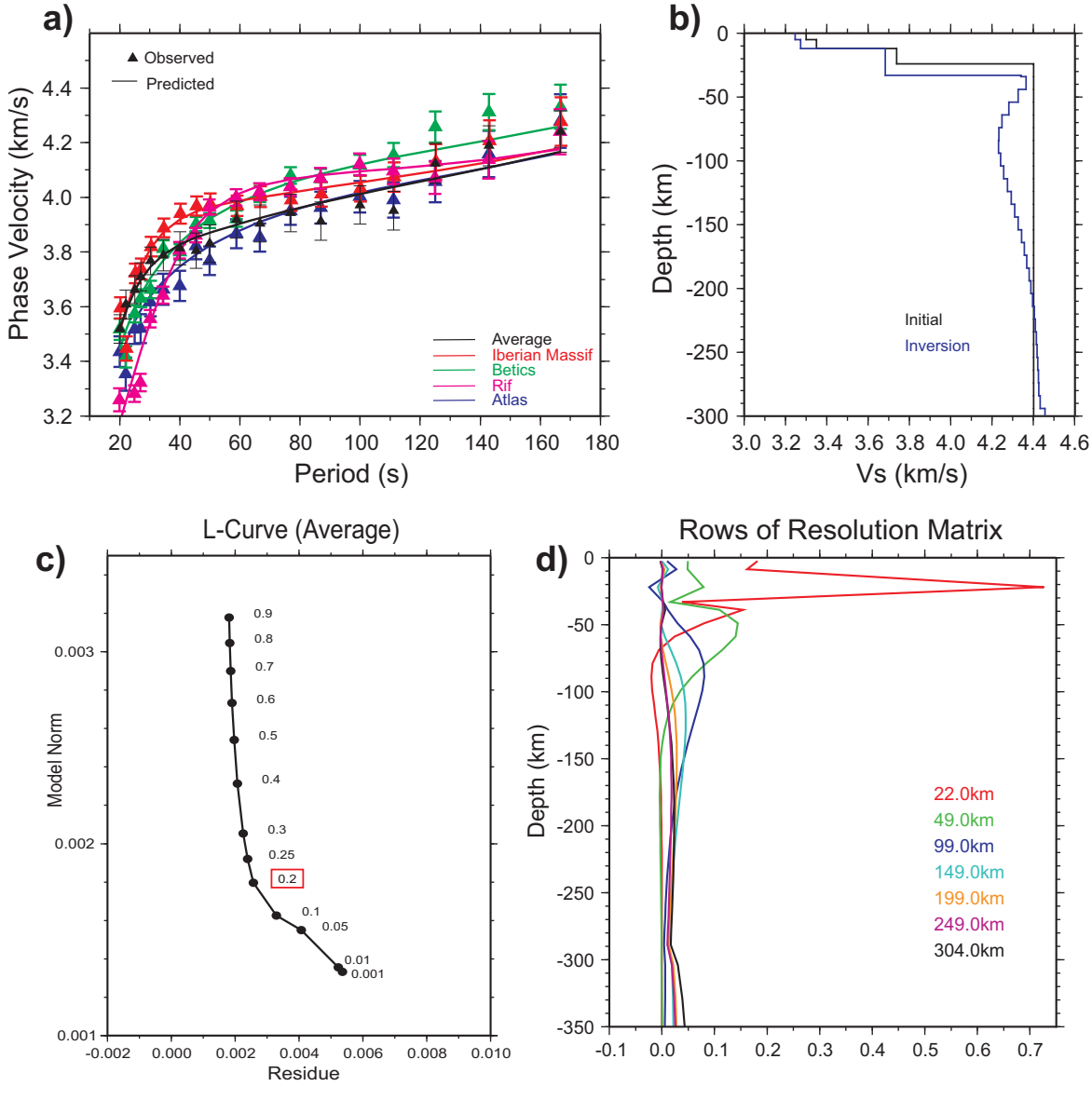

Figure 3. (a) Predicted dispersion curve (solid line) for the average phase velocities (triangles) of the different tectonic areas. (b) Average Vs model (blue) inverted from the starting model (black) to fit the dispersion curve in Figure 3a. (c) L curve of the Vs model norm and residuals of the phase velocity prediction for the estimation of the damping parameter. (d) Rows of the resolution matrix for depths of 22, 49, 99, 149, 199, 249, and 304 km.

were windowed for each period with variable length tapered windows in order to isolate the fundamental mode Rayleigh waves from higher-order modes and body waves (Figure 2b). Amplitude was corrected for the frequency-dependent anelastic attenuation and geometrical spreading [*Mitchell*, 1995]. The observed amplitudes were then normalized to the root mean square (RMS) amplitude for each event to remove earthquake magnitude variations. The distribution of events and stations gives good ray coverage in the whole area (Figure 2c), with over 8000 raypaths at almost every period (Figure 2d). As a number of the stations were deployed for only part of this period, or were moved during the recording period, no event was recorded by all 228 stations but no fewer than 135 events per period were used (Figure 2d).

[14] We obtained the shear velocity structure in a two-step procedure: first we calculated the 2-D phase velocity for each period using the modified two-plane wave technique as described in *Forsyth and Li* [2005] and *Yang and Forsyth* [2006b]. We then inverted the dispersion curve to get the shear

velocities. This technique has been successfully applied to obtain the phase velocity and azimuthal structures in other regions [e.g., *Yang and Forsyth*, 2006a; *Miller et al*., 2009; *Wagner et al*., 2010; *Liu et al*., 2011]. The two-plane waves technique allows the use of complex waveforms associated with the multipathed arrival of energy and with Rayleigh waves arriving off the great circle path due to scattering between the source and receiver outside of the study area. For each period, the observed waveforms are modeled as the sum of two distinct plane waves of unknown amplitude, initial phase, and propagation direction, with these six parameters describing the incoming primary and scattered wavefield. The area is parameterized by 841 nodes on an evenly distributed 0.5° × 0.5° grid exceeding the receiver-covered region by 1.5°. These peripheral grid nodes have larger a priori standard deviation to absorb traveltime residuals of the wave not well resolved by the two-plane waves representation. The amplitude and phase variations resulting from the interference of these two-plane waves are first inverted using a simulated annealing method to establish the best fitting parameters for the two-plane waves. In a second step, the six parameters at each grid node are calculated simultaneously in a generalized linear inversion [*Tarantola and Valette*, 1982] to determine 2-D phase velocities across the study area. In this step, both the phase delay and amplitude effects of local structure are calculated using finite-frequency kernels [*Yang and Forsyth*, 2006b] to increase lateral resolution. In order to smooth the sensitivity kernels, a Gaussian weighted function is used with a characteristic length (L) of 65 km. This parameter controls the trade-off between model resolution and model variance. In our inversion, we choose $L = 65$ km following *Liu et al*. [2011] because of similar station spacing in both studies. To test the resolution of lateral phase velocity variations we generated synthetic Rayleigh wave data with the real data geometry from a checkerboard model (see supporting information[1]). The checkerboard pattern is well recovered in most of the investigated area covered by the stations in almost all periods. Nonetheless, the pattern fades at longer periods.

[16] The resulting phase velocity dispersion curves (Figure 3a) are inverted using the nonlinear least squares DISPER80 code [*Saito*, 1988] to obtain a 1-D shear velocity-depth function at every point on a uniform 0.25° grid. As an initial model for the inversion, we used a single upper mantle layer with Vs = 4.4 km/s, and a three layer crust with Vs chosen to be consistent with the Vp structure determined from active source experiment in the Betics, Atlas, and Iberian Massif (Figure 3b). The density and the Vp/Vs ratio are kept fixed in each layer. The initial crustal thickness is constrained by the results from [*Fullea et al*., 2010]. The inversion was run with a suite of damping parameters, the overall best damping was 0.2 based on an L test comparing model energy versus RMS error (Figure 3c). The 3-D Vs model is the collection of the 1-D Vs-depth functions.

[17] To evaluate the resolution of the shear wave velocity model, we examine the rows of the 1-D reference model resolution matrix at different layers calculated from the inversion matrix (Figure 3d). At shallow depths the peak of the rows of the resolution matrix are well localized in depth (e.g., 22 and 50 km). The peaks of the resolution matrix for greater depths gradually become broader and decrease in value, indicating that the number of adjacent layers needed to recover one entire piece of independent information of the model increases with depth. In our analysis, the pick can still be recognized at ∼250 km indicating that the shear velocity model is well resolved to this depth.

4. Phase Velocity Maps

[18] The resulting phase velocity maps (Figure 4) show strong lateral variations at the shorter periods (≤45 s) that correlate well with geological structures. At periods less than 45 s, the lowest phase velocities are found in the Gibraltar Strait and surrounding area, with variation from the mean greater than 10%. Low phase velocities are also observed beneath the Betics and Rif at periods between 20 to 30 s, indicating a thicker crust than the surrounding areas. Other areas with low phase velocities at short periods ($T < 40$ s) are the High and Middle Atlas but in these areas the low phase velocities persist up to periods of 100 s, suggestive of a thin lithosphere. Higher-phase velocities are observed beneath the Iberian Massif, the Alboran Sea, and Moroccan Meseta.

5. 3-D Shear Velocity Model

[19] The shear velocity model (Figure 5) shows relatively rapid variations in shear velocity

[1]Additional supporting information may be found in the online version of this article.

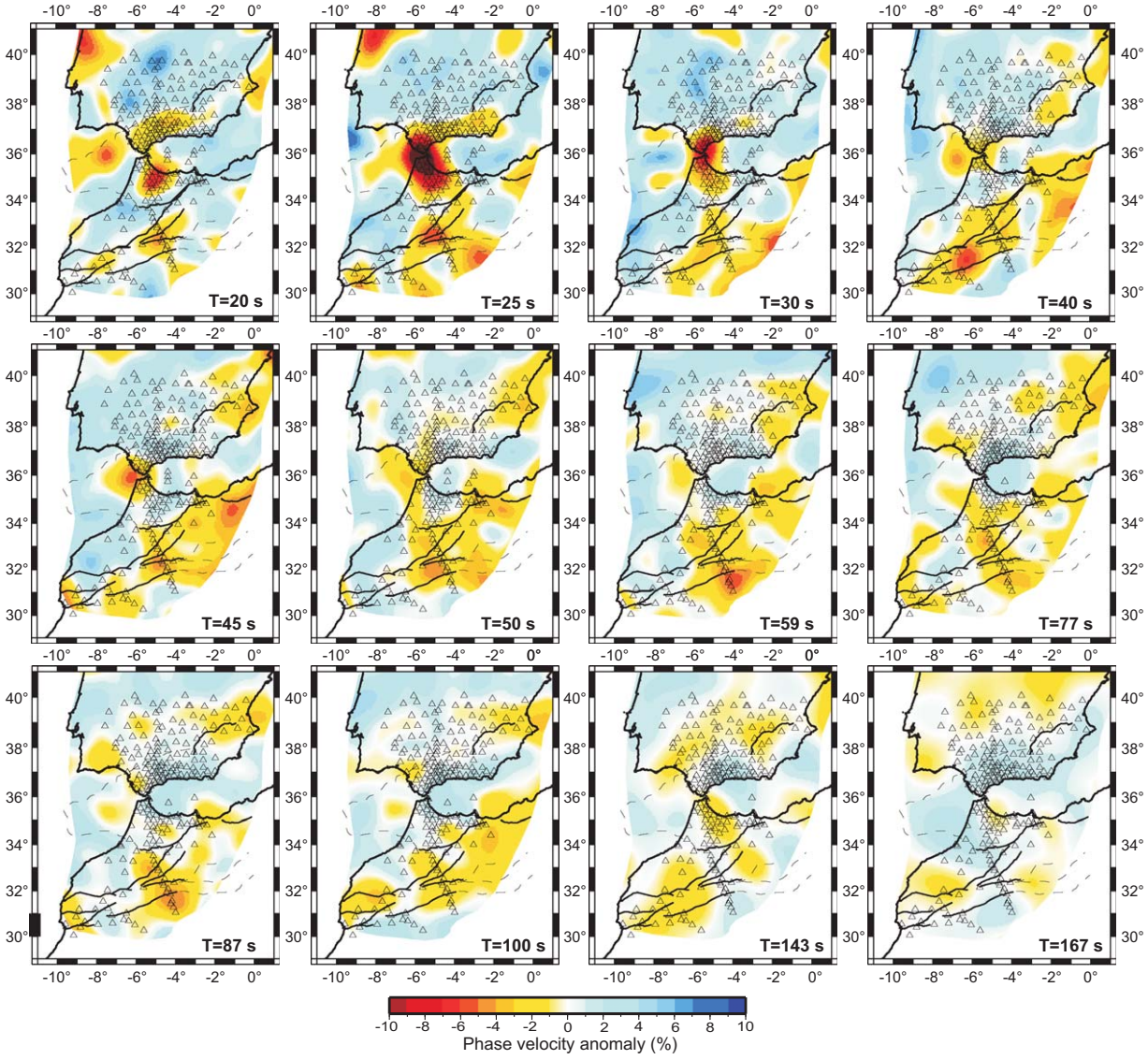

Figure 4. Rayleigh wave phase velocity anomaly maps. The plotted phase velocity anomaly is referred to the average phase velocity at each period. Open triangles represent the stations used. Tectonic boundaries are shown as black lines.

between the difference tectonic provinces to ~150 km depth, and significant differences between the Alboran Sea region and its surroundings persisting to 230 km. Although having 20 s as the shortest period in the inversion allows little control on the shallow to midcrustal velocities, we still observe large differences in the bulk crustal shear velocity which vary laterally with geologic structures (Figure 5).

5.1. Iberian Massif

[20] The Iberian Massif has quite homogenous crustal shear velocity (Figures 5 and 6a). On average, the velocity is ~3.6 km/s in the middle and lower crust. Around 33 km depth velocity increases to 4.3 km/s. No remarkable crustal differences are observed between the tectonic provinces forming the Massif. In the uppermost mantle, velocity increases progressively with depth up to ~4.5 km/s at ~70 km depth. At ~80 km depth, velocity starts to decrease. This pattern is observed in all of the Iberian Massif except in the Calatrava volcanic field, a small area at 4°W and 38.75°N (Figures 5, 6e, 7 and section 3) where low shear velocities (~4.3 km/s) are observed as shallower as ~65 km. We interpret these shallow low upper mantle velocities as the source region of the late Miocene-late Pliocene volcanism.

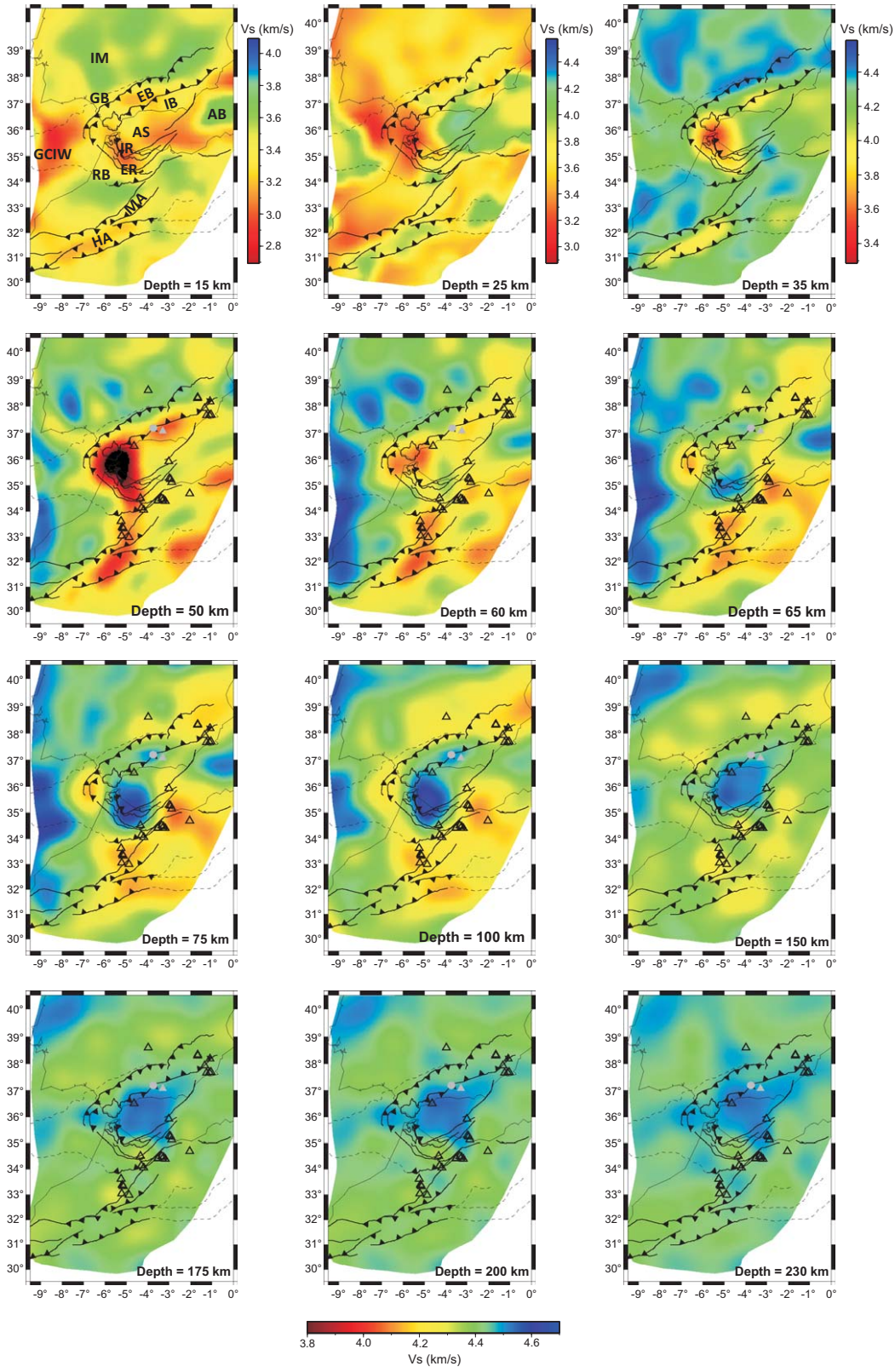

Figure 5. Maps of absolute shear velocity at different depths. Gray triangle represents the Sierra Nevada Mountains and the gray dot the Granada Basin. Tectonic boundaries are shown as black lines. (top) Different color scale is used for each crustal depth. A common color scale is used for upper mantle depths.

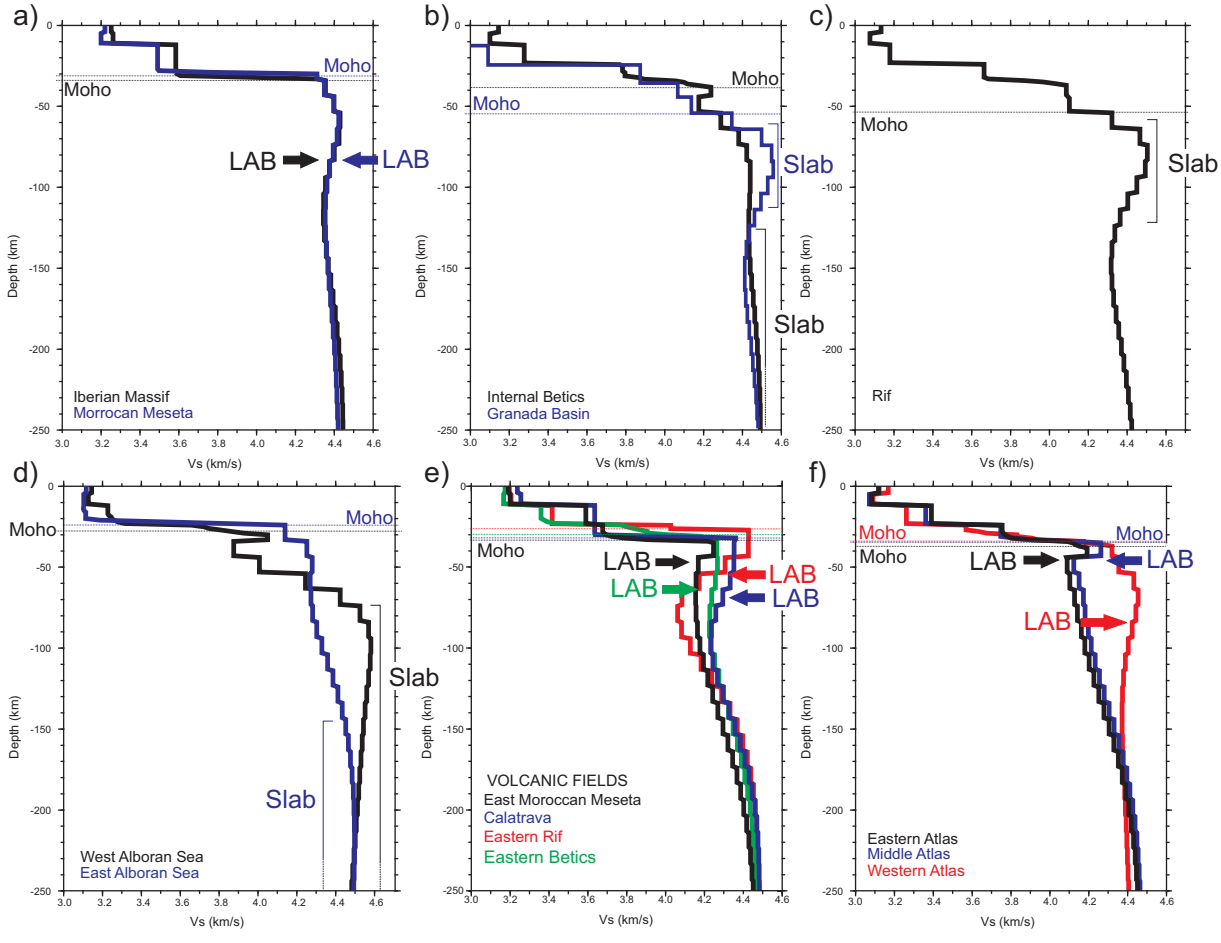

Figure 6. 1-D average shear velocity for the different regions of the area. Moho depth is represented by a dashed line. The estimated LAB depth shown in Figure 10 and the high Vs interpreted as the western Mediterranean Slab are indicated.

5.2. Gibraltar Arc and Alboran Sea

[21] The Gibraltar Arc is built of the Betic and Rif Mountains. Even though they are part of the same mountain system with similar litho-tectonic units, the two ranges show different crustal shear velocities (Figures 5 and 6). The middle and lower crustal shear velocities obtained in the Rif are slightly lower than in the Betics. In the Betics at 15 km depth the average velocity is 3.3 km/s while in the Rif at the same depth is 3.2 km/s. In the Betics velocity increases to 3.8 km/s from 25 to 33–35 km depth where velocity jumps to 4.2 km/s (Figure 6b). Velocity increases gradually to 4.4 km/s at ~80 km depth, then remains almost constant with depth. This pattern is observed throughout the internal Betics, with the notable exception of the Granada Basin and the Sierra Nevada Mountains. There at 25 km depth the shear velocity is 3.9 km/s increasing to 4.0 km/s at 35 km depth, with the jump to velocities over 4.2 km/s at 55 km depth (Figure 6b). Velocity then increases with depth to ~4.6 km/s at ~75 km, remaining almost up to 100 km depth. There is a 4% velocity reversal centered at ~150 km depth with velocities again reaching 4.5 km/s at 250 km depth.

[22] In the Rif Mountains, similar pattern than beneath the Granada Basin is observed. From 25 km depth, velocity increases with depth from 3.6 to 4.1 km/s at 55 km (Figure 6c), the depth of the Moho estimated from recent seismic refraction measurements [*Gallart et al.*, 2012]. From this depth, velocity increases rapidly to almost 4.6 km/s by ~65 km depth. Below 95 km, velocity decreases to 4.3 km/s at 150 km depth (Figure 6c). The same low velocity (3.6 km/s) is observed in the Strait of Gibraltar, to ~60 km depth, with an increase to 4.4 km/s to ~75 km depth where it increases again to 4.6 km/s.

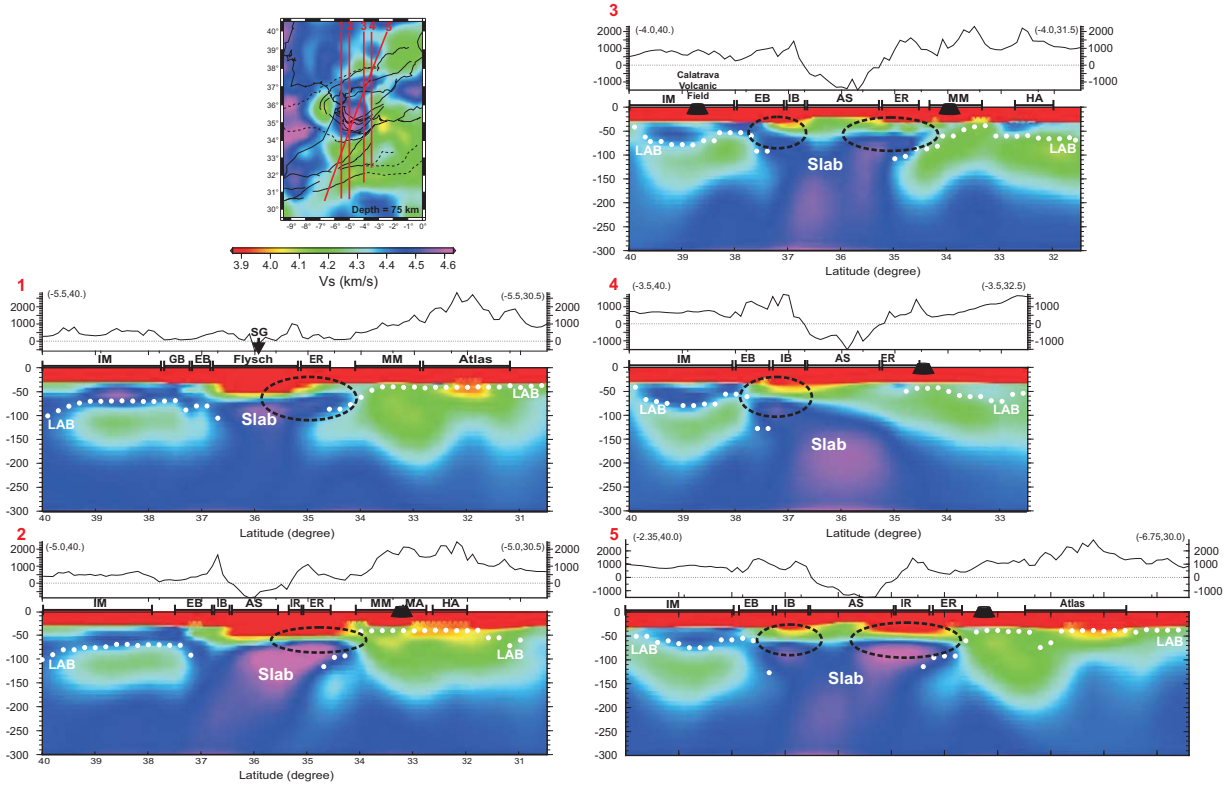

Figure 7. NS absolute Vs cross sections crossing the Iberian Massif, the Gibraltar Arc, and the Atlas Mountains indicated on the velocity map at 75 km depth. The crustal velocity is set to a constant 3.9 km/s to enhance mantle anomalies. Tectonic provinces are indicated (IM: Iberian Massif; EB: External Betics; IB: Internal Betics; AS: Alboran Sea; ER: External Rif; IR: Internal Rif; MM: Moroccan Meseta; MA: Middle Atlas; HA: High Atlas; GC: Gulf of Cadiz; SG: Strait of Gibraltar). Black cones represent the position of Cenozoic volcanic eruptions. White dots show the depth of the estimated LAB (see text and Figure 10). Black dashed ellipses indicate where the western Mediterranean Slab is still attached to the lower crust.

[23] The upper mantle velocity structure of the eastern and western Alboran Sea is remarkably different. In both, the Alboran Sea crustal velocities are low (<3.2 km/s) to almost 20 km depth. In the east Alboran Sea, velocity sharply increases to >4.1 km/s increasing steadily with depth to >4.5 km/s at 90 km depth (Figure 6d). In the westernmost Alboran Sea at ~20 km depth, velocity increases to ~4.0 km/s, then reverses to ~3.9 km/s at 40 km depth. It then rapidly increases with depth to 4.6 km/s at 75 km and remains almost constant with depth (Figure 6d).

5.3. Moroccan Meseta

[24] The shear velocity model for the Moroccan Meseta is similar to the one obtained for the Iberian Massif (Figure 6a). On average at 15 km depth the velocity is 3.5 km/s. This velocity remains constant down to ~32 km depth where it increases steeply to 4.3 km/s. Then velocity increases with depth to >4.4 km/s centered at 55–75 km depth. A mild velocity reversal, to 4.3 km/s, is centered at 110–120 km depth. From here velocity again increases with depth up to 4.4 km/s at 250 km depth. Between the Rharb Basin and the Middle Atlas under the eastern Moroccan Meseta, mantle shear velocities are lower than in the overall Moroccan Meseta (Figure 6e). Velocity is around 4.1 km/s at 45 km depth and slightly increases to 4.2 km/s at 130 km depth. These low velocities appear beneath a middle Miocene-late Pliocene basaltic volcanic field. The low upper mantle velocities are likely the source region for these basalts.

5.4. Atlas Mountains

[25] The shear velocity model shows differences between the High and Middle Atlas, and the western Atlas (Figure 6f). At 15 km depth, shear velocity beneath the High and Middle Atlas is ~3.4 km/s (Figures 5 and 6) increasing to 3.7 km/s at ~25 km. In both, the Middle and High Atlas, the

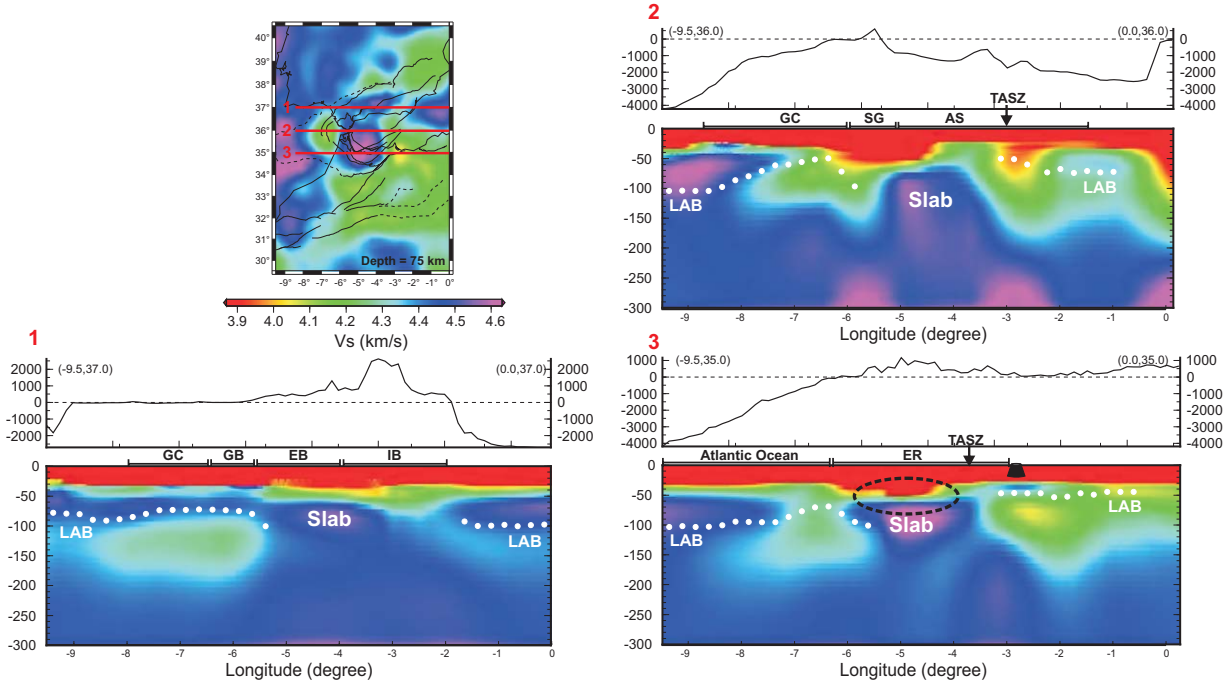

Figure 8. EW absolute Vs cross sections along the Gibraltar Arc indicated on velocity map at 75 km depth map. Velocities less than 3.9 km/s are set to a constant 3.9 km/s to enhance mantle anomalies. Tectonic provinces are indicated (EB: External Betics; IB: Internal Betics; AS: Alboran Sea; ER: External Rif; GC: Gulf of Cadiz; SG: Strait of Gibraltar). Black arrow indicates where the sections cross the Trans Alboran Shear Zone (TASZ). Black cones represent the position of Cenozoic volcanics. White dots indicate the depth of the estimated LAB (see text and Figure 10). Black dashed ellipses indicate where the slab is attached to the lower crust.

velocity of the mantle just below the Moho (~35 km depth) increases to ~4.3 km/s, forming a thin mantle lid to about 45 km depth where velocity reverses, decreasing to ~4.1 km/s. Beneath the low-velocity zone, the velocity gradually increases with depth being >4.4 km/s at ~250 km depth.

[26] Slightly lower velocities are observed in the crust of the western Atlas at 15 km depth (3.3 km/s) than in the High Atlas. Then velocity increases from 3.3 km/s at 25 km depth to ~4.3 km/s at ~35 km depth. From here velocity increases to almost 4.5 km/s at 65 km depth. There is a >3% decreases in velocity centered at 140 km depth.

5.5. LAB Depth Estimation

[27] The LAB is usually a second-order discontinuity that separates the conductive, rigid, dry, and chemically depleted lithosphere from the convective, mechanically weak, often hydrated, fertile, and possibly partially molten asthenosphere [*Fischer et al.*, 2010]. In seismology the LAB is usually associated with a shear velocity reversal below the upper mantle lid. We have estimated the LAB depth as the depth of the maximum negative shear velocity gradient lying below the fast lid. We calculated the vertical Vs gradient from the velocity model and mapped the maximum negative gradient as the LAB (Figures 6–10).

[28] The resulting map (Figure 10) shows strong lateral changes in LAB topography, with depths as shallow as ~40 km to deeper than 110 km. In general, our LAB map presents shallower estimates of the LAB depth than previous estimates made from geopotential field modeling [*Fernàndez et al.*, 2004; *Teixell et al.*, 2005; *Zeyen et al.*, 2005; *Missenard et al.*, 2006; *Fullea et al.*, 2010; *Palomeras et al.*, 2011]. Our results place the lithosphere-asthenosphere boundary beneath the Iberian Massif at ~85 km depth, shallowing to ~50 km toward the northeast. A similar LAB depth is obtained beneath the eastern External Betics. Beneath the westernmost Alboran Domain where the western Mediterranean high velocity anomaly starts its descent from the crust to the transition zone, there is no LAB in the sense defined above. We would not identify the lithosphere as being 600+ km deep, but instead note that seismology does not

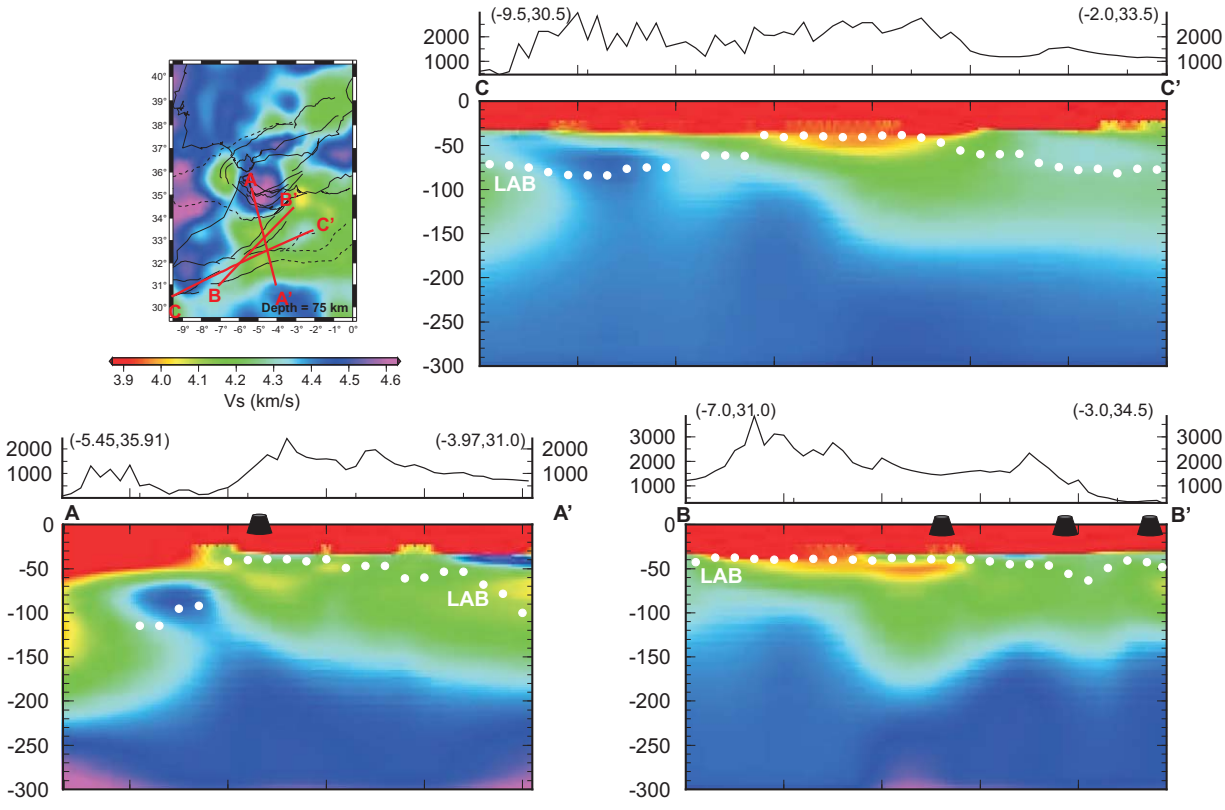

Figure 9. Cross sections through the Atlas Mountains indicated on the Vs map at 75 km depth. The crustal velocities less than 3.9 km/s are is to a constant 3.9 km/s for display. Horizontal segments represent the tectonic zones (ER: External Rif; MM: Moroccan Meseta; MA: Middle Atlas; HA: High Atlas). Black cones represent the position of Cenozoic volcanics. White dots indicate the depth of the estimated LAB (see text and Figure 10).

provide a useful observation for estimating lithosphere depth at the location of pronounced lithospheric downwellings.

[29] A shallow LAB is also mapped beneath the eastern Moroccan Meseta, and parts of the Middle and High Atlas, with the lithosphere in places being only 45–50 km thick. The LAB deepens to 85–90 km under the western Atlas and the western Moroccan Meseta. It is worth noting that under the intraplate Cenozoic Calatrava volcanic field the estimated depth of the LAB is as shallow as 60 km, and beneath the Cenozoic volcanic fields in Morocco it is at 45–50 km. The estimate of the LAB depth in the western Mediterranean is an important constraint to the geodynamic evolution of the region.

6. Discussion

[30] Shear velocity models have been previously obtained for the crust and upper mantle of Europe and the Mediterranean region by body wave tomography [e.g., *Schmid et al.*, 2008], surface wave tomography [e.g., *Peter et al.*, 2008; *Boschi et al.*, 2009; *Schivardi and Morelli*, 2009], adjoint inversion applied to surface waves, and body wave data [*Legendre et al.*, 2012; *Zhu et al.*, 2012] as well as surface waves and gravity data [*Tondi et al.*, 2012]. As these models cover large areas and use relatively widely spaced seismograph stations, they have low lateral resolution. In contrast, the relatively dense broadband array (Dx $\leq$ 60 km) available in this study and the finite-frequency kernels used for estimating phase velocities provide a laterally well-resolved model.

6.1. Western Mediterranean High Velocity Anomaly Beneath the Alboran Domain

[31] As described above, a number of different scenarios have been proposed to explain the evolution of the Mediterranean basin and in particular the western Mediterranean. Some models are based on slab rollback [*Lonergan and White*,

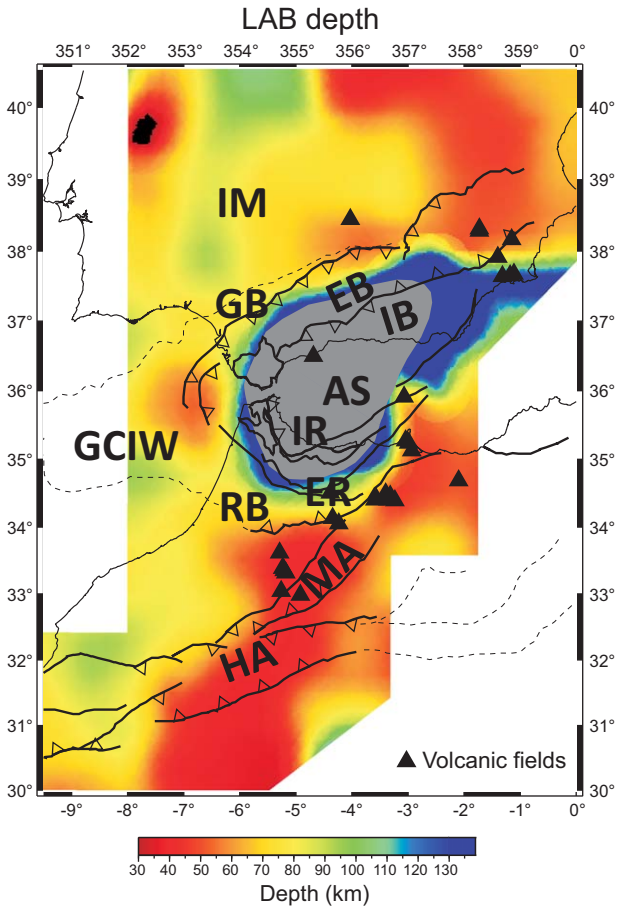

Figure 10. LAB depth estimates calculated from the greatest negative vertical velocity gradient (see text). Gray area indicates the limits of high velocities (>4.5 km/s) at 100 km depth. Black triangles are the position of the volcanics fields.

1997; *Gutscher et al.*, 2002; *Rosenbaum et al.*, 2002] and others on mantle lithospheric instability [*Platt and Vissers*, 1989; *Seber et al.*, 1996a; *Calvert et al.*, 2000]. *P* wave tomography studies show a high velocity east dipping anomaly beneath the Alboran Sea [*Gutscher et al.*, 2002; *Spakman and Wortel*, 2004; *Bezada et al.*, 2013], extending from shallow depths to the transition zone. This anomaly is interpreted as the subducting westernmost Mediterranean oceanic lithosphere. SKS splitting [*Díaz et al.*, 2010] and dispersion of body waves measurements [*Bokelmann and Maufroy*, 2007; *Bokelmann et al.*, 2011] support the subduction rollback model. Our results also show high velocities (~4.6 km/s) beneath the Rif from ~65 to ~110 km depth dipping to the north (Figures 7 and 11) and from this depth dipping to the east (Figures 8 and 11). A smaller high-velocity area is also mapped beneath the Granada Basin, at 4°W and 37°N, dipping south from ~70 km depth. At ~110 km depth, both high-velocity areas merge into a larger anomaly that extends beneath the Rif, western Alboran Sea and internal Betics (Figures 5 and 11). Recent *P* wave tomography [*Bezada et al.*, 2013] also shows two branches of the slab in the upper most mantle with essentially the same geometry described. This high-velocity body descends almost vertically to depths greater than 250 km in the surface wave image. Combined with the *P* wave tomography image [*Bezada et al.*, 2013] the feature can be seen to Transition Zone depths beneath the Alboran Sea. We interpret this high-velocity continuous body as the slab of the Tethys' oceanic lithosphere subducted beneath Eurasia.

[32] In contrast to this high-velocity feature centered under the Gibraltar Arc and western Alboran Sea, low upper mantle shear velocities are mapped both surrounding it and overlying much of it beneath the Alboran Sea. Low velocities in the upper mantle are typically interpreted as resulting from higher temperatures, possible partial melt or oriented seismic anisotropy, or any combination of these factors. The average heat flow in the Alboran Sea increases from west to east from values of ~69 to ~124 mWm^{-2} [*Polyak et al.*, 1996], indicative of high temperatures in the eastern Alboran where continental crust has been thinned to less than 20 km. The presence of Miocene magmatism on the Alboran seafloor indicates the presence of partial melt. Geochemical studies of Alboran Miocene volcanics suggest they are due to back-arc extension associated with slab rollback [*Duggen et al.*, 2004; *Gill et al.*, 2004]. This suggests that the low velocities beneath the Alboran Sea are related to the induced corner flow in the asthenospheric mantle wedge produced above the slab.

6.2. Attached Slab and Lithosphere Removal

[33] One important question that bears on evolutionary models of the Gibraltar Arc orogeny is whether or not the slab currently forms part of an active subduction zone. Body wave tomography does not have resolution at depths shallower than 150–200 km therefore it cannot resolve whether the slab is attached or not [e.g., *Calvert et al.*, 2000]. The shear velocity model shows low velocities (~3.8 km/s) in the Gibraltar Strait and vicinity (Figures 5, 7, and 8), down to ~55 km depth, overlying the high mantle velocities that we interpret as the slab. Velocities of 3.8 km/s are typical of crustal lithologies, despite there being no

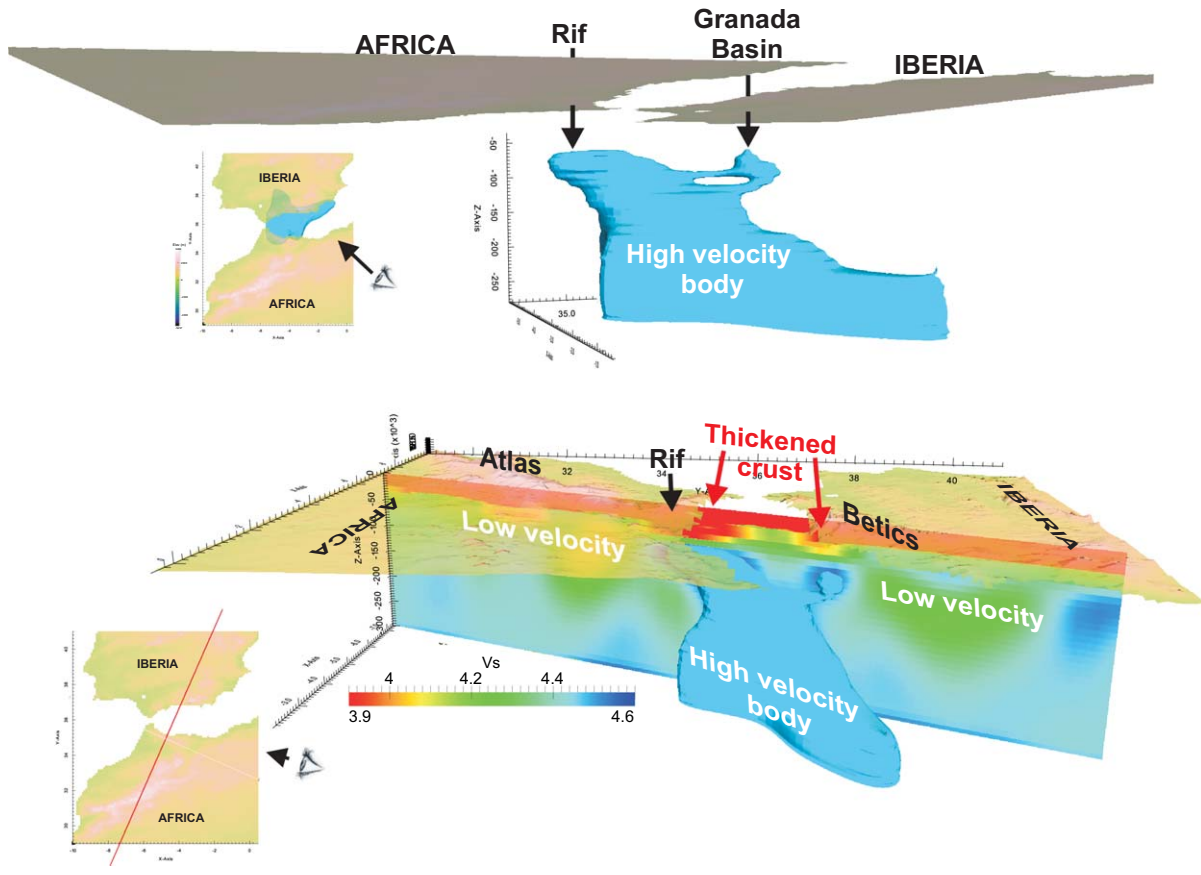

Figure 11. 3-D view of the high interpreted as a slab beneath the western Mediterranean. (top) The shape of the slab defined by the 4.5 km/s isosurface. Beneath the Rif the slab dips to the north, beneath the Betics it dips south, where the two join the slab dips toward the east. Inset shows the view of the high-velocity volume from the top. (bottom) Same high-velocity isovolume from another angle of view with a slice of the shear velocity model, showing the relation of the high-velocity isovolume with surrounding low shear velocities. Inset marks the position of the shear velocity slice (red line).

topographic suggestion of such a thick crust. The base of these low velocities have been mapped as the Moho from PmP reflections in a recent wide-angle experiment in the Rif [*Gallart et al*., 2012], and correspond to a strong positive arrival in Ps receiver functions [*Mancilla et al*., 2012; *Thurner et al*., in press]. As the base of the mapped low crustal velocities is coincident with the top of the high velocities, we propose that the slab is locally attached to the crust of the Alboran Domain beneath the Rif. The observed thick crust could be the consequence of the sinking slab depressing the continental crust in this region. We note that a recent study of Global Positioning System (GPS) velocities in the southern Iberia and northern Morocco conclude that the slab must still be attached to the base of the Rif in this same area [*Perouse et al*., 2010; *Vernant et al*., 2010].

[34] Beneath the Betics at ~4°W and 37°N (Figures 7 and 8) crustal velocities are also observed down to >50 km depth. At this location a second branch of high velocities emanating from the main body is observed at depths as shallow as 65–70 km. This is either still attached to the crust, is currently detaching from the crust, or has recently separated from the bottom of the crust. We also note that the shallow to intermediate depth seismicity under the Betics is found near the top of this feature (Figure 5), presenting the intriguing possibility that the slab is in the process of detaching. The seismicity and the uplift of the Sierra Nevada, as opposed to the relatively modest elevations in the Rif, cause us to favor the latter two hypotheses, that the slab is either still detaching or has recently detached.

[35] Beneath the Strait of Gibraltar, we observe also a thick crust (>55 km), but here the top of the high velocities appears ~15 km deeper than the bottom of the crust. Therefore, we conclude that the slab was attached in the recent past, pulling

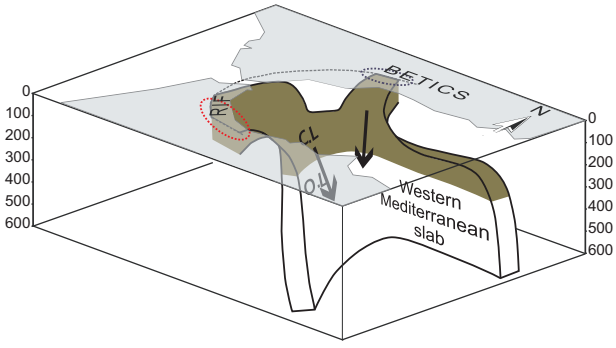

Figure 12. Simplified 3-D geometry of the western Mediterranean high-velocity slab based on the surface wave tomography study, modified from *Perouse et al*. [2010]. In the model, the sinking slab is still attached to the crust beneath the Rif Mountains (red dashed ellipse) and is currently detaching beneath the Granada Basin (blue dashed ellipse), removing the continental lithospheric mantle under southern Spain (C.L., brown domain); O.L.: oceanic lithosphere (white domain). Black arrow is the pull of the oceanic part of the slab (O.L.) at depth.

down the crust in the same way that it is doing at present in the Rif.

[36] The geodynamic model that we propose for the western Mediterranean based on the shear velocity model is summarized in Figure 12. To us the observations that the descending slab is still attached to the crust beneath the Rif, and was recently attached to the crust of the Betics beneath the Granada Basin suggest a more complex subduction scenario than simple slab rollback. *Gutscher et al*. [2012] proposed a similar scenario where the slab detachment began ~5 Ma. In addition to including the mantle formerly beneath the Alboran Domain and any oceanic lithosphere lying between the Alboran Domain and the current Gibraltar Arc, the slab is also removing the lithospheric mantle of the continental margins beneath both Iberia and Morocco. This lithospheric removal is associated with thickening of the crust up to 55 km depth in the places where the slab is still attached (Rif) or recently detached (Sierra Nevada and Strait of Gibraltar). The lithospheric removal appears to control the development of topography along both continental margins, as seen in the recent rapid uplift of the Sierra Nevada as well as the active extension in the Granada Basin. We also think, as other authors have proposed [e.g., *Duggen et al*., 2005; *Bezada et al*., 2013], that the slab has removed the lithosphere from beneath the Alboran Sea during rollback. The lithosphere has subsequently been replaced by asthenospheric material as is inferred by the low shear velocities observed. The shear velocity model also correlates well with the evolution of the magmas in the Betics and Rif that evolve from arc volcanism during the Middle to Late Miocene, to alkaline volcanism during Late Miocene to Quaternary [*Duggen et al*., 2004].

6.3. The Atlas

[37] Beneath the eastern High and Middle Atlas we observe low shear velocities in the upper mantle (Figures 7 and 9) with the LAB at very shallow depths (~50 km), in contrast to the western Atlas, where the LAB is ~80 km (Figure 10). These shallow low velocities lie in a corridor between 6°W and 5°W and extend to the north into the eastern Moroccan Meseta, beneath Cenozoic volcanic fields (Figures 1, 7, and 9). Shear velocities are as low as 4.0 km/s at 60 km depth and 4.2 km/s at 140 km depth. Regional *P* wave tomography by *Seber et al*. [1996b] also indicates low velocities in the upper most mantle in this area. Several studies modeling geopotential fields and heat flow suggest a thin lithosphere beneath the Middle and High Atlas [*Zeyen et al*., 2005; *Missenard et al*., 2006; *Fullea et al*., 2010] to explain the relatively low Bouguer gravity anomaly (−120 mGal) and a high geoid anomaly (16 m) in this mountain range. This interpretation is consistent with our results, suggesting that at least part of the Middle and High Atlas is underlain by an asthenosphere at shallow (~50 km) depths (Figure 10) with mantle buoyancy helping to support the topography not related to shortening.

6.4. Cenozoic volcanism

[38] Cenozoic volcanism occurred across this region. The geochemical composition of these volcanic rocks appears to be related to subduction in the Alboran Sea [e.g., *Gill et al*., 2004] and to Si-poor intraplate magmatism in SW-Iberia [e.g., *Cebriá and López-Ruiz*, 1995] and Morocco [e.g., *Duggen et al*., 2005]. Pronounced low shear velocities in the upper mantle are well correlated with many of the intraplate basaltic volcanic fields. In these regions shear velocities decrease by more than 7% relative to the surrounding mantle. This reduction in Vs could be caused by a 1% melt fraction according to *Hammond and Humphreys* [2000] or by a 2% melt fraction according to *Takei* [2000]. This reduction in Vs could also be caused by an increase in temperature of 300–400°K [*Karato*, 1993; *Cammarano et al*., 2003].

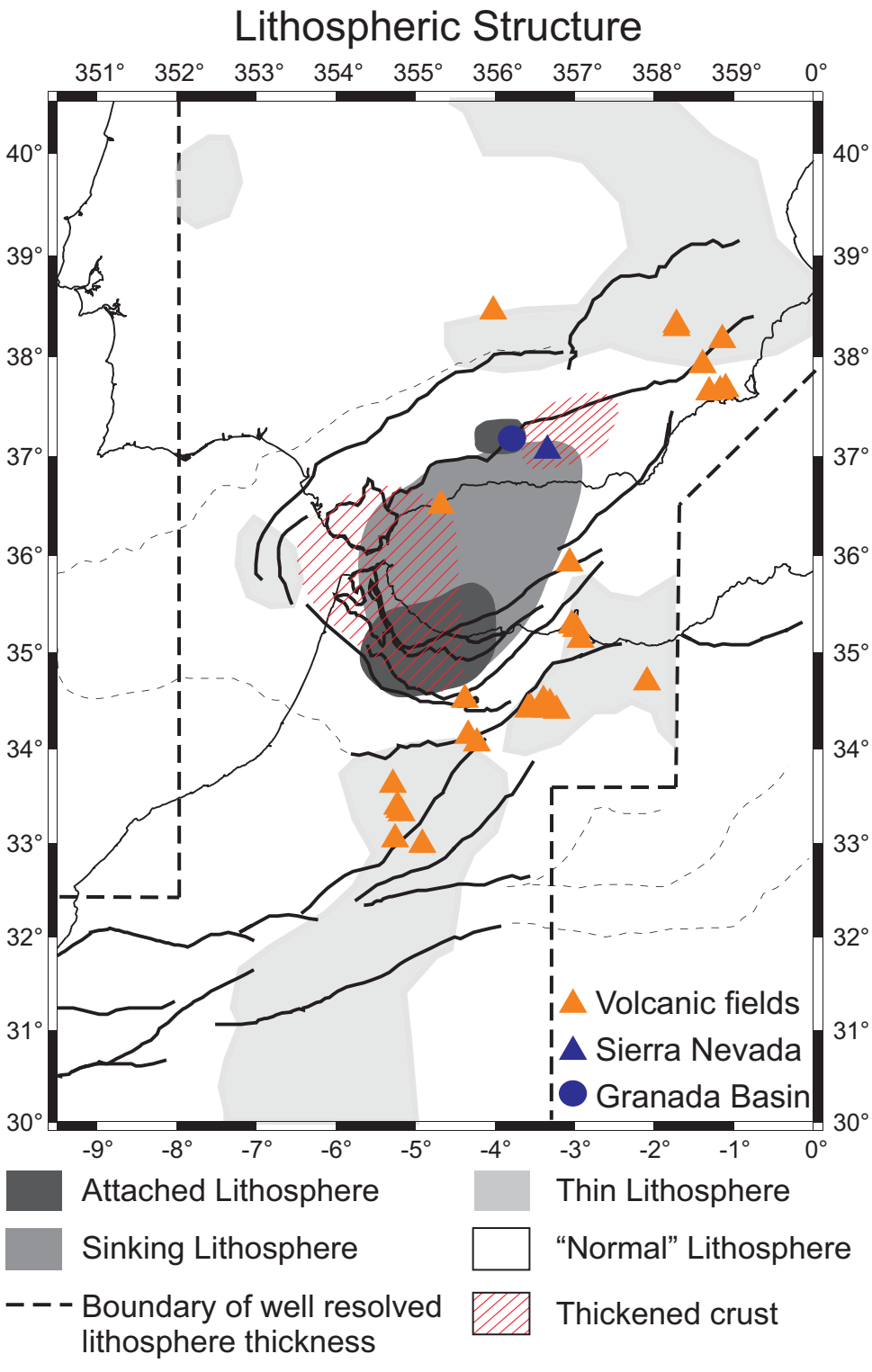

Figure 13. Lithospheric structure for the western Mediterranean inferred from this surface wave tomography study.

Consequently, we believe that the low velocities indicate the presence of high temperatures and/or partial melt that was the source for some of these magmas.

[39] Back-arc magmatism is concentrated in the Alboran Domain. Uppermost mantle velocities in this region are also low (4.2 km/s) above ~70 km depth, above a rapid increase that marks the top of

the slab. We attribute these low velocities above the slab as asthenospheric flow produced in the mantle wedge during slab retreat.

[40] Beneath the Neogene Calatrava volcanic field (Spain) the overall average Iberian LAB (~85 km depth) shallows to ~65 km depth (Figure 10) with velocities we identify as asthenosphere (4.2 km/s) at ~70 km depth, shallower than elsewhere under the Iberian Massif (Figure 7). This shallow low velocity may be the remnant source of the magmatism, since geochemical studies suggest it melted at depths shallower than 100 km [*Humphreys et al*., 2010].

[41] In the Atlas and Moroccan Meseta we also observed low (4.1 km/s) uppermost mantle velocities beneath relatively large Miocene basalt flows (Figures 7 and 9). In this area the low velocities are seen throughout the whole mantle beneath the Moho. The estimated LAB depth is as shallow as 45 km beneath these volcanics.

7. Conclusions

[42] The finite-frequency Rayleigh wave tomography results, obtained from dense station coverage (~240 stations from a variety of different permanent and temporary networks) provides a detailed 3-D shear velocity model for the western Mediterranean to ~250 km depth. The model shows dramatic vertical and lateral velocity differences that we can relate to outcrop geology at shallow depths, and to larger, mantle-scale geodynamic features at greater depths.

[43] We have observed significant differences in the lithospheric structure of the Iberian Massif, the Alboran Domain, and Atlas Mountains that are summarized in Figure 13. The most important feature is the high-velocity (>4.5 km/s) western Mediterranean slab extending from ~75 km depth beneath the Alboran Domain, which is still attached to the crust under the Rif Mountains to the south and is still attached or has recently detached from the Betic Mountains to the north and northeast (Figures 11 and 12). Evidence for this are the low velocities (<3.8 km/s) mapped down to 60 km depth beneath the Rif, just above the high shear velocity slab anomaly, supported by evidence from dense regional Ps receiver functions [*Thurner et al*., in press], refraction/wide-angle seismology in the Rif [*Gallart et al*., 2012], and recent interpretations of geodetic data [*Perouse et al*., 2010]. We suggest that the slab that has rolled back beneath the Alboran Domain also removes some or all of the continental margin mantle lithosphere from the adjacent continents as it descends into the mantle, controlling topography along both the Iberian and Moroccan continental margins (Figure 12).

[44] The velocity model has unusually low upper mantle shear velocities directly beneath the Atlas, giving rise to a very shallow LAB. A low-density upper mantle provides support for the high elevations of the Atlas. We also have identified relatively shallow low upper mantle shear velocities as the sources of different types of Cenozoic volcanism under this region.

Acknowledgments

[45] This research was funded by the U.S. National Science Foundation EAR-0808939. The deployment of the IberArray broadband seismic network is part of the CONSOLIDER CSD2006-00041 (Geosciences in Iberia: Integrated studies on Topography and 4-D Evolution) grant from the Spanish Ministry of Science and Innovation. Additional funding was provided by the Spanish ministry under grants CGL2010-17280 and by Generalitat de Catalunya under grant 2009 SGR 6. We thank the IRIS data management center, the Instituto Geografico Nacional (Spain), the Instituto de Meteorologia (Portugal), the Centro de Geofisica da Universidade de Lisboa (Portugal), the Universidad Complutense de Madrid (Spain), and the University of Muenster (Germany) for contributing data to this study. Thanks to the Seismology and Tectonics at Rice (STAR) group for valuable discussions.

References

Arboleya, M. L., A. Teixell, M. Charroud, and M. Julivert (2004), A structural transect through the High and Middle Atlas of Morocco, *J. Afr. Earth Sci.*, *39*(3–5), 319–327, doi: 10.1016/j.jafrearsci.2004.07.036.

Ayarza, P., et al. submitted, Crustal thickness and velocity structure across the Moroccan Atlas from long offset wide-angle reflection seismic data: The SIMA experiment, *Geochem. Geophys. Geosyst*.

Beauchamp, W., R. W. Allmendinger, M. Barazangi, A. Demnati, M. El Alji, and M. Dahmani (1999), Inversion tectonics and the evolution of the High Atlas Mountains, Morocco, based on a geological-geophysical transect, *Tectonics*, *18*(2), 163–184.

Bezada, M. J., E. D. Humphreys, D. R. Toomey, M. Harnafi, and J. M. Davila (2013), Evidence for slab rollback in westernmost Mediterranean from improved upper mantle imaging, *Earth Planet. Sci. Lett.*, *368*, 51–60.

Blanco, M. J., and W. Spakman (1993), The P-wave velocity structure of the mantle below the Iberian Peninsula: Evidence for subducted lithosphere below southern Spain, *Tectonophysics*, *221*, 13–34.

Bokelmann, G., and E. Maufroy (2007), Mantle structure under Gibraltar constrained by dispersion of body waves,

Geophys. Res. Lett., *34*, L22305, doi:10.1029/2007GL030964.

Bokelmann, G., E. Maufroy, L. Buontempo, J. Morales, and G. Barruol (2011), Testing oceanic subduction and convective removal models for the Gibraltar arc: Seismological constraints from dispersion and anisotropy, *Tectonophysics*, *502*(1–2), 28–37, doi:10.1016/j.tecto.2010.08.004.

Boschi, L., B. Fry, G. Ekström, and D. Giardini (2009), The European upper mantle as seen by surface waves, *Surv. Geophys.*, *30*(4–5), 463–501, doi:10.1007/s10712-009-9066-2.

Buforn, E., A. Udias, and R. Madariaga (1991), Intermediate and deep earthquakes in Spain, *Pure Appl. Geophys.*, *136*(4), 375–393.

Buontempo, L., G. H. R. Bokelmann, G. Barruol, and J. Morales (2008), Seismic anisotropy beneath southern Iberia from SKS splitting, *Earth Planet. Sci. Lett.*, *273*(3–4), 237–250, doi:10.1016/j.epsl.2008.06.024.

Calvert, A., E. Sandvol, D. Seber, M. Barazangi, S. Roecker, T. Mourabit, F. Vidal, G. Alguacil, and N. Jabour (2000), Geodynamic evolution of the lithosphere and upper mantle beneath the Alboran region of the western Mediterranean: Constraints from travel time tomography, *J. Geophys. Res.*, *105*(B5), 10,871–10,898.

Cammarano, F., S. Goes, P. Vacher, and D. Giardini (2003), Inferring upper-mantle temperatures from seismic velocities, *Phys. Earth Planet. Inter.*, *138*(3–4), 197–222, doi:10.1016/S0031-9201(03)00156-0.

Carbonell, R., V. Sallares, J. Pous, J. J. Danobeitia, P. Queralt, J. J. Ledo, and V. Garcia Duenas (1998), A multidisciplinary geophysical study in the Betic chain (southern Iberian Peninsula), *Tectonophysics*, *288*(l), 137–152.

Cebriá, J.-M., and J. López-Ruiz (1995), Alkali basalts and leucitites in an extensional intracontinental plate setting: The late Cenozoic Calatrava Volcanic Province (central Spain), *Lithos*, *35*(1–2), 27–46, doi:10.1016/0024-4937(94)00027-Y.

Díaz, J., and J. Gallart (2009), Crustal structure beneath the Iberian Peninsula and surrounding waters: A new compilation of deep seismic sounding results, *Phys. Earth Planet. Inter.*, *173*(1–2), 181–190, doi:10.1016/j.pepi.2008.11.008.

Díaz, J., A. Villaseñor, J. Gallart, J. Morales, A. Pazos, D. Cordoba, J. A. Pulgar, J. L. García Lobón, M. Harnafi, and T. S. W. Group (2009), The IBERARRAY broadband seismic network: A new tool to investigate the deep structure beneath Iberia, *Orfeus Newsl.*, *8*(2), 1–6.

Díaz, J., J. Gallart, A. Villaseñor, F. de L. Mancilla, A. Pazos, D. Córdoba, J. A. Pulgar, P. Ibarra, and M. Harnafi (2010), Mantle dynamics beneath the Gibraltar Arc (western Mediterranean) from shear-wave splitting measurements on a dense seismic array, *Geophys. Res. Lett.*, *37*, L18304, doi:10.1029/2010GL044201.

Duggen, S., K. Hoernle, P. van den Bogaard, and C. Harris (2004), Magmatic evolution of the Alboran region: The role of subduction in forming the western Mediterranean and causing the Messinian Salinity Crisis, *Earth Planet. Sci. Lett.*, *218*(1–2), 91–108, doi:10.1016/S0012-821X(03)006 32-0.

Duggen, S., K. Hoernle, P. van den Bogaard, and D. Garbe-Schonberg (2005), Post-collisional transition from subduction- to intraplate-type magmatism in the westernmost Mediterranean: Evidence for continental-edge delamination of subcontinental lithosphere, *J. Petrol.*, *46*(6), 1155–1201, doi:10.1093/petrology/egi013.

Durand, B., L. Jolivet, F. Horvath, and M. Seranne (Eds.) (1999), *The Mediterranean Basins: Tertiary Extension within the Alpine Orogen*, Geol. Soc., London.

Faccenna, C., C. Piromallo, A. Crespo-Blanc, L. Jolivet, and F. Rossetti (2004), Lateral slab deformation and the origin of the western Mediterranean arcs, *Tectonics*, *23*, TC1012, doi:10.1029/2002TC001488.

Fernàndez, M., I. Marzán, and M. Torne (2004), Lithospheric transition from the Variscan Iberian Massif to the Jurassic oceanic crust of the Central Atlantic, *Tectonophysics*, *386*(1–2), 97–115, doi:10.1016/j.tecto.2004.05.005.

Fischer, K. M., H. A. Ford, D. L. Abt, and C. A. Rychert (2010), The lithosphere-asthenosphere boundary, *Ann. Rev. Earth Planet. Sci.*, *38*(1), 551–575, doi:10.1146/annurev-earth-040809-152438.

Forsyth, D. W., and A. Li (2005), Array-analysis of two-dimensional variations in surface wave phase velocity and azimuthal anisotropy in the presence of multipathing interference, in *Seismic Earth: Array Analysis of Broadband Seismograms*, edited by A. Levander and G. Nolet, pp. 81–97, AGU, Washington, D. C.

Fullea, J., M. Fernàndez, J. C. Afonso, J. Vergés, and H. Zeyen (2010), The structure and evolution of the lithosphere–asthenosphere boundary beneath the Atlantic–Mediterranean Transition Region, *Lithos*, *120*(1–2), 74–95, doi:10.1016/j.lithos.2010.03.003.

Gallart, J., A. Gil, J. Díaz, M. Harnafi, A. Levander, I. Palomeras, and D. Cordoba (2012), Variations of the crustal structure in the Rif Cordillera, N-Morocco, from wide-angle seismic data, Abstract presented at 2012 Fall Meeting, AGU, San Francisco, Calif. Abstract T32D-05.

Gill, R. C. O., A. Aparicio, M. El Azzouzi, J. Hernandez, M. F. Thirlwall, J. Bourgois, and G. F. Marriner (2004), Depleted arc volcanism in the Alboran Sea and shoshonitic volcanism in Morocco: Geochemical and isotopic constraints on Neogene tectonic processes, *Lithos*, *78*(4), 363–388, doi:10.1016/j.lithos.2004.07.002.

Grimison, N. L., and W. Chen (1986), The Azores-Gibraltar plate boundary: Focal mechanisms, depths of earthquakes, and their tectonic implications, *J. Geophys. Res.*, *91*(B2), 2029–2047.

Gutscher, M. A., J. Malod, J.-P. Rehault, I. Contrucci, F. Klingelhoefer, L. Mendes-Victor, and W. Spakman (2002), Evidence for active subduction beneath Gibraltar, *Geology*, *30*(12), 1071–1074, doi:10.1130/0091-7613(2002)030<1071.

Gutscher, M. A., et al. (2012), The Gibraltar subduction: A decade of new geophysical data, *Tectonophysics*, *574–575*, 72–91, doi:10.1016/j.tecto.2012.08.038.

Hammond, W. C., and E. D. Humphreys (2000), Upper mantle seismic wave velocity: Effects of realistic partial melt geometries, *J. Geophys. Res.*, *105*(B5), 10,975–10,986, doi:10.1029/2000JB900041.

Humphreys, E. R., K. Bailey, C. J. Hawkesworth, F. Wall, J. Najorka, and A. H. Rankin (2010), Aragonite in olivine from Calatrava, Spain: Evidence for mantle carbonatite melts from >100 km depth, *Geology*, *38*(10), 911–914, doi:10.1130/G31199.1.

Jacobshagen, V., K. Gorler, and P. Giese (1988), Geodynamic evolution of the Atlas System (Morocco) in post-Palaeozoic times, in *The Atlas System of Morocco: Studies on Its Geodynamic Evolution, Lecture Notes Earth Sci.*, edited by V. Jacobshagen, pp. 481–499, Springer, New York.

Jiménez-Munt, I., M. Fernàndez, J. Vergés, D. Garcia-Castellanos, J. Fullea, M. Pérez-Gussinyé, and J. C. Afonso (2011), Decoupled crust-mantle accommodation of Africa-Eurasia convergence in the NW Moroccan margin, *J. Geophys. Res.*, *116*, B08403, doi:10.1029/2010JB008105.

Karato, S. (1993), Importance of anelasticity in the interpretation of seismic tomography, *Geophys. Res. Lett.*, *20*(15), 1623–1626.

Koulali, A., D. Ouazar, A. Tahayt, R. W. King, P. Vernant, R. E. Reilinger, S. McClusky, T. Mourabit, J. M. Davila, and N. Amraoui (2011), New GPS constraints on active deformation along the Africa–Iberia plate boundary, *Earth Planet. Sci. Lett.*, *308*(1–2), 211–217, doi:10.1016/j.epsl.2011.05.048.

Laville, E., and J.-P. Petit (1984), Role of synsedimentary strike-slip faults in the formation of Moroccan Triassic basins, *Geology*, *12*(7), 424–427, doi:10.1130/0091-7613(1984)12<424.

Legendre, C. P., T. Meier, S. Lebedev, W. Friederich, and L. Viereck-Götte (2012), A shear wave velocity model of the European upper mantle from automated inversion of seismic shear and surface waveforms, *Geophys. J. Int.*, *191*, 282–304, doi:10.1111/j.1365-246X.2012.05613.x.

Liu, K., A. Levander, F. Niu, and M. S. Miller (2011), Imaging crustal and upper mantle structure beneath the Colorado Plateau using finite frequency Rayleigh wave tomography, *Geochem. Geophys. Geosyst.*, *12*, Q07001, doi:10.1029/2011GC003611.

Lonergan, L., and N. White (1997), Origin of the Betic-Rif mountain belt, *Tectonics*, *16*(3), 504–522.

López-Ruiz, J., J. M. Cebria, M. Doblas, R. Oyarzun, M. Hoyso, and C. Martin (1993), Cenozoic intra-plate volcanism related to extensional tectonics at Calatrava, central Iberia, *J. Geol. Soc. London*, *150*, 915–922.

Malinverno, A., and W. B. F. Ryan (1986), Extension in the Tyrrhenian Sea and shortening in the Apennines as result of arc migration driven by sinking of the lithosphere, *Tectonics*, *5*(2), 227–245.

Mancilla, F. D. L., et al. (2012), Crustal thickness variations in northern Morocco, *J. Geophys. Res.*, *117*, B02312, doi:10.1029/2011JB008608.

Martínez-Martínez, J. M., G. Booth-Rea, J. M. Azañón, and F. Torcal (2006), Active transfer fault zone linking a segmented extensional system (Betics, southern Spain): Insight into heterogeneous extension driven by edge delamination, *Tectonophysics*, *422*(1–4), 159–173, doi:10.1016/j.tecto.2006.06.001.

Martínez Poyatos, D., et al. (2012), Imaging the crustal structure of the Central Iberian Zone (Variscan Belt): The ALCUDIA deep seismic reflection transect, *Tectonics*, *31*, TC3017, doi:10.1029/2011TC002995.

Matte, P. (1986), Tectonics and plate tectonics model for the Variscan belt of Europe, *Tectonophysics*, *126*, 329–374.

Matte, P. (2001), The Variscan collage and orogeny (480–290 Ma) and the tectonic definition of the Armorica microplate: A review, *Terra Nova*, *13*, 122–128.

Miller, M. S., A. Levander, F. Niu, and A. Li (2009), Upper mantle structure beneath the Caribbean-South American plate boundary from surface wave tomography, *J. Geophys. Res.*, *114*, B01312, doi:10.1029/2007JB005507.

Missenard, Y., H. Zeyen, D. Frizon de Lamotte, P. Leturmy, C. Petit, M. Sébrier, and O. Saddiqi (2006), Crustal versus asthenospheric origin of relief of the Atlas Mountains of Morocco, *J. Geophys. Res.*, *111*, B03401, doi:10.1029/2005JB003708.

Mitchell, B. J. (1995), Anelastic structure and evolution of the continental crust and upper mantle from seismic surface wave attenuation, *Rev. Geophys.*, *33*(4), 441–462.

Morales, J., I. Serrano, A. Jabaloy Sánchez, J. Galindo-Zaldívar, D. Zhao, F. Torcal, F. Vidal, and F. Gonzalez-Lodeiro (1999), Active continental subduction beneath the Betic Cordillera and the Alborán Sea, *Geology*, *27*, 735–738, doi:10.1130/0091-7613(1999)027<0735.

Palomeras, I., R. Carbonell, I. Flecha, F. Simancas, P. Ayarza, J. Matas, D. Martínez Poyatos, A. Azor, F. González-Lodeiro, and A. Pérez-Estaún (2009), Nature of the lithosphere across the Variscan orogen of SW Iberia: Dense wide-angle seismic reflection data, *J. Geophys. Res.*, *114*, B02302, doi:10.1029/2007JB005050.

Palomeras, I., R. Carbonell, P. Ayarza, M. Fernàndez, J. F. Simancas, D. Martinez Poyatos, F. González Lodeiro, and A. Pérez-Estaún (2011), Geophysical model of the lithosphere across the Variscan Belt of SW-Iberia: Multidisciplinary assessment, *Tectonophysics*, *508*(1–4), 42–51, doi:10.1016/j.tecto.2010.07.010.

Perouse, E., P. Vernant, J. Chery, R. Reilinger, and S. McClusky (2010), Active surface deformation and sublithospheric processes in the western Mediterranean constrained by numerical models, *Geology*, *38*(9), 823–826, doi:10.1130/G30963.1.

Peter, D., L. Boschi, F. Deschamps, B. Fry, G. Ekström, and D. Giardini (2008), A new finite-frequency shear-velocity model of the European-Mediterranean region, *Geophys. Res. Lett.*, *35*, L16315, doi:10.1029/2008GL034769.

Piromallo, C., and A. Morelli (2003), P wave tomography of the mantle under the Alpine-Mediterranean area, *J. Geophys. Res.*, *108*(B2), 2065, doi:10.1029/2002JB001757.

Platt, J. P., and R. L. M. Vissers (1989), Geology Extensional collapse of thickened continental lithosphere: A working hypothesis for the Alboran Sea and Gibraltar arc, *Geology*, *17*, 540–543, doi:10.1130/0091-7613(1989)017<0540.

Polyak, B. G., et al. (1996), Heat flow in the Alboran Sea, western Mediterranean, *Tectonophysics*, *263*, 191–218.

Rosenbaum, G., G. S. Lister, and C. Duboz (2002), Reconstruction of the tectonic evolution of the western Mediterranean since the Oligocene, *J. Virtual Explor.*, *8*, 107–130.

Royden, L. H. (1993), Evolution of retreating subduction boundaries formed during continental collision, *Tectonics*, *12*(3), 629–638.

Saito, M. (1988), DISPER80: A subroutine package for the calculation of seismic normal-mode solutions, in *Seismological Algorithms: Computational Methods and Computer Programs*, edited by D. J. Doornbos, pp. 293–319, Academic, San Diego, Calif.

Schivardi, R., and A. Morelli (2009), Surface wave tomography in the European and Mediterranean region, *Geophys. J. Int.*, *177*(3), 1050–1066, doi:10.1111/j.1365-246X.2009.04100.x.

Schmid, C., S. van der Lee, J. C. VanDecar, E. R. Engdahl, and D. Giardini (2008), Three-dimensional S velocity of the mantle in the Africa-Eurasia plate boundary region from phase arrival times and regional waveforms, *J. Geophys. Res.*, *113*, B03306, doi:10.1029/2005JB004193.

Schwarz, G., and P. J. Wigger (1988), Geophysical studies of the Earth's Crust and Upper Mantle in the Atlas System of Morocco, in *The Atlas System of Morocco: Studies on its Geodynamic Evolution, Lecture Notes Earth Sci.*, edited by V. Jacobshagen, pp. 339–357, Springer, New York.

Seber, D., M. Barazangi, A. Ibenbrahim, and A. Demnati (1996a), Geophysical evidence for lithospheric delamination beneath the Alboran Sea and Rif-Betic mountains, *Nature*, *379*, 785–790.

Seber, D., M. Barazangi, B. A. Tadili, M. Ramdani, A. Ibenbrahim, and D. Ben Sari (1996b), Three-dimensional upper mantle structure beneath the intraplate Atlas and

interplate Rif mountains of Morocco, *J. Geophys. Res.*, *101*(B2), 3125–3138.

Simancas, J. F., et al. (2003), Crustal structure of the transpressional Variscan orogen of SW Iberia: SW Iberia deep seismic reflection profile (IBERSEIS), *Tectonics*, *22*(6), 1062, doi:10.1029/2002TC001479.

Spakman, W., and R. Wortel (2004), A Tomographic View on Western Mediterranean Geodynamics, in *The TRANSMED Atlas: The Mediterranean Region From Crust to Mantle.*, edited by W. Cavazza et al., pp. 31–52, Springer, Berlin.

Surinach, E., and R. Vegas (1988), Lateral inhomogeneities of the Hercynian crust in central Spain, *Phys. Earth Planet. Inter.*, *51*, 226–234.

Takei, Y. (2000), Acoustic properties of partially molten media studied on a simple binary system with a controllable dihedral angle, *J. Geophys. Res.*, *105*(B7), 16,665–16,682, doi:10.1029/2000JB900124.

Tarantola, A., and B. Valette (1982), Generalized nonlinear inverse problems solved using the least squares criterion, *Rev. Geophys.*, *20*(2), 219–232, doi:10.1029/RG020i002p00219.

Teixell, A., M. L. Arboleya, M. Julivert, and M. Charroud (2003), Tectonic shortening and topography in the central High Atlas (Morocco), *Tectonics*, *22*(5), 1051, doi:10.1029/2002TC001460.

Teixell, A., P. Ayarza, H. Zeyen, M. Fernandez, and M.-L. Arboleya (2005), Effects of mantle upwelling in a compressional setting: The Atlas Mountains of Morocco, *Terra Nova*, *17*(5), 456–461, doi:10.1111/j.1365-3121.2005.00633.x.

Thurner, S., I. Palomeras, A. Levander, and R. Carbonell (in press), Evidence for Ongoing Lithospheric Removal in the Western Mediterranean: Ps Receiver Functions Results From the PICASSO Project, *Geochem. Geophys. Geosyst*.

Timoulali, Y., and M. Meghraoui (2011), 3-D crustal structure in the Agadir region (SW High Atlas, Morocco), *J. Seismol.*, *15*(4), 625–635, doi:10.1007/s10950-011-9240-0.

Tondi, R., R. Schivardi, I. Molinari, and A. Morelli (2012), Upper mantle structure below the European continent: Constraints from surface-wave tomography and GRACE satellite gravity data, *J. Geophys. Res.*, *117*, B09401, doi:10.1029/2012JB009149.

Vernant, P., A. Fadil, T. Mourabit, D. Ouazar, A. Koulali, J. M. Davila, J. Garate, S. McClusky, and R. Reilinger (2010), Geodetic constraints on active tectonics of the Western Mediterranean: Implications for the kinematics and dynamics of the Nubia-Eurasia plate boundary zone, *J. Geodyn.*, *49*(3–4), 123–129, doi:10.1016/j.jog.2009.10.007.

Wagner, L., D. W. Forsyth, M. J. Fouch, and D. E. James (2010), Detailed three-dimensional shear wave velocity structure of the northwestern United States from Rayleigh wave tomography, *Earth Planet. Sci. Lett.*, *299*(3–4), 273–284, doi:10.1016/j.epsl.2010.09.005.

Wigger, P., G. Asch, P. Giese, W.-D. Heinsohn, S. O. El Alami, and F. Ramdani (1992), Crustal structure along a traverse across the Middle and High Atlas mountains derived from seismic refraction studies, *Geol. Rundsch.*, *81*(1), 237–248.

Wortel, M. J. R., and W. Spakman (2000), Subduction and slab detachment in the Mediterranean-Carpathian region, *Science*, *290*(5498), 1910–1917, doi:10.1126/science.290.5498.1910.

Yang, Y., and D. W. Forsyth (2006a), Rayleigh wave phase velocities, small-scale convection, and azimuthal anisotropy beneath southern California, *J. Geophys. Res.*, *111*, B07306, doi:10.1029/2005JB004180.

Yang, Y., and D. W. Forsyth (2006b), Regional tomographic inversion of the amplitude and phase of Rayleigh waves with 2-D sensitivity kernels, *Geophys. J. Int.*, *166*(3), 1148–1160, doi:10.1111/j.1365-246X.2006.02972.x.

Zeyen, H., P. Ayarza, M. Fernàndez, and A. Rimi (2005), Lithospheric structure under the western African-European plate boundary: A transect across the Atlas Mountains and the Gulf of Cadiz, *Tectonics*, *24*, TC2001, doi:10.1029/2004TC001639.

Zhu, H., E. Bozdağ, D. Peter, and J. Tromp (2012), Structure of the European upper mantle revealed by adjoint tomography, *Nat. Geosci.*, *5*, 493–498, doi:10.1038/ngeo1501.